Report 13, 1991

TEMPERATURE DISTRIBUTION AND SIMULATION OF THE BODMODSSTADIR GEOTHERMAL FIELD IN SOUTHERN ICELAND

Wang Liangshu,
UNU Geothermal Training Programme,
Orkustofnun - National Energy Authority,
Grensásvegur 9,
108 Reykjavík,
ICELAND

Permanent address:
Department of Earth Sciences,
Nanjing University,
Nanjing 210008,
P. R. CHINA

ABSTRACT

The Bodmodsstadir geothermal field is one of the low temperature geothermal fields located just outside the neovolcanic zone in southern Iceland. Ten wells have been drilled in this area since 1974. Well BS-1 is the only producer and the water from it is used for greenhouses and space heating at the Bodmodsstadir farm. The formation temperature distribution in the area, the location of aquifers and a conceptual model of the geothermal field are presented in this report. This study is based on temperature logs, water level measurements and pressure in the wells and other geological and geophysical data. To further develop the model of the Bodmodsstadir geothermal system, both steady-state and non-steady-state simulations were performed. When assuming a fracture situated between wells BS-2 and BS-10, dipping 8° and striking N40°E in the steady-state simulation, the calculated temperature distribution matches well the observed temperature in the wells. The non-steady-state simulation indicates that it took about 5000 years for this system to reach quasi-steady-state (natural state). Furthermore, when solving both the mass and the energy transport equations in the non-steady-state simulation, the recharge rate from depth has to be in the range of 1-10 kg/s, with permeability of the fracture between 0.1-0.8 Darcy to match the observed temperature data. The natural state model developed in this study could be used to evaluate this geothermal system and for planning its development.

TABLE OF CONTENTS

LIST OF FIGURES

LIST OF TABLES

1. INTRODUCTION

The constructive boundaries between the North American and Eurasian plates follow the Mid-Atlantic Ridge and cross Iceland from southwest to northeast (Palmason, 1973). In Iceland the boundaries are characterized by a central zone of rifting and volcanic activity. During the processes of rifting and volcanic activity, heat energy is transported into the crust and high and low temperature geothermal systems are formed. Some of these geothermal systems have been prospected and exploited.

Bodmodsstadir low temperature field is one of the geothermal systems in southern Iceland. Two wells were drilled there in 1974 and since then the first one has been producing boiling water for local greenhouse and space heating. Eight more wells were drilled during the summer 1991. This report primarily emphasizes the question of the origin and natural state of the Bodmodsstadir geothermal field and is based on temperature data, water level and pressure, soil temperature measurements and other data.

Most of the geothermal systems in Iceland are convective systems connected to near-vertical macroscopic fractures which are, in many cases, associated with faults, or dykes. Fractures greatly increase the permeability of the basaltic formations and provide paths for the geothermal fluids. The main features of a convective geothermal system, such as temperature, pressure and direction of the flow, depend on the strike, dip and scale of the fracture. Consequently, this report first focuses on the existence of a possible fracture at depth that could explain the character of the Bodmodsstadir geothermal field (conceptual model), then on the simulation of temperature distribution around the fracture using different initial and boundary conditions. By comparing the simulation results with formation temperatures measured in boreholes, the strike and dip of the fracture can be estimated in order to obtain valuable information for the reconnaissance and exploitation of the Bodmodsstadir geothermal field.

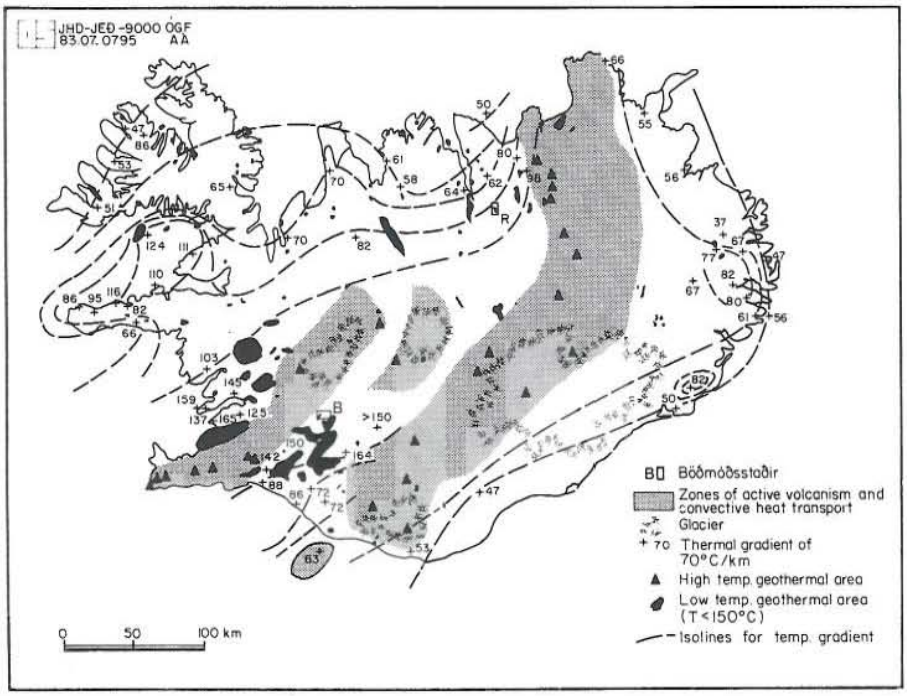

FIGURE 1: The regional temperature gradient and the distribution of geothermal activity in Iceland (Flovenz, 1985). The location of the Bodmodsstadir geothermal field is inferred with the letter B.

2. GENERAL ASPECTS OF THE GEOTHERMAL FIELD

2.1 Location and geological setting

The Bodmodsstadir low temperature geothermal field is located in southern Iceland (Figures 1 and 2), about 60 km east of Reykjavík and about 3 km northeast of the lake Apavatn. The river, Brúará, flowing southwards, forms the southern boundary of the geothermal area. Its area is about 0.06 km^2. All the wells were surveyed by Gunnar Thorbergsson (1991) and the coordinates are shown in Table 1. Figure 3 shows the topography of the Bodmodsstadir area based on these data. The surface elevation is from 66 m to 72 m above sea level with the northwestern part higher than the southeastern part.

A zone of active volcanism crosses central Iceland (Figure 1). This active volcanic zone represents the extension and accretion of the crust. Basaltic magma raised from the asthenosphere erupts and intrudes intensively so that the crust beneath this rifting zone is very hot. In some places, such as at Krafla (Bodvarsson et al., 1984) and Nesjavellir (Bodvarsson et al., 1990), magma bodies are located at a few kilometres depth in the crust. The rifting processes transport heat energy into the crust so that the rift zone has become a zone where high temperature geothermal fields occur. On both sides are zones of low temperature fields. The rift zone is split into two branches in south Iceland and the Bodmodsstadir geothermal field is located between the two branches. The Bodmodsstadir field is, therefore, closely related to the rifting processes in the Mid-Atlantic Ridge.

At the border of the active volcanic zone, the temperature gradient is very high, over 150°C/km. As can be seen in Figure 1, the regional temperature gradient at Bodmodsstadir is also very high.

According to the geological map of Iceland (sheet 6, 1:250000), the Bodmodsstadir region is covered by till and alluvium, the first of which was deposited beneath the glacier and the second deposited in the front of a glacier. It is about 50 m thick as has been revealed by drilling. A

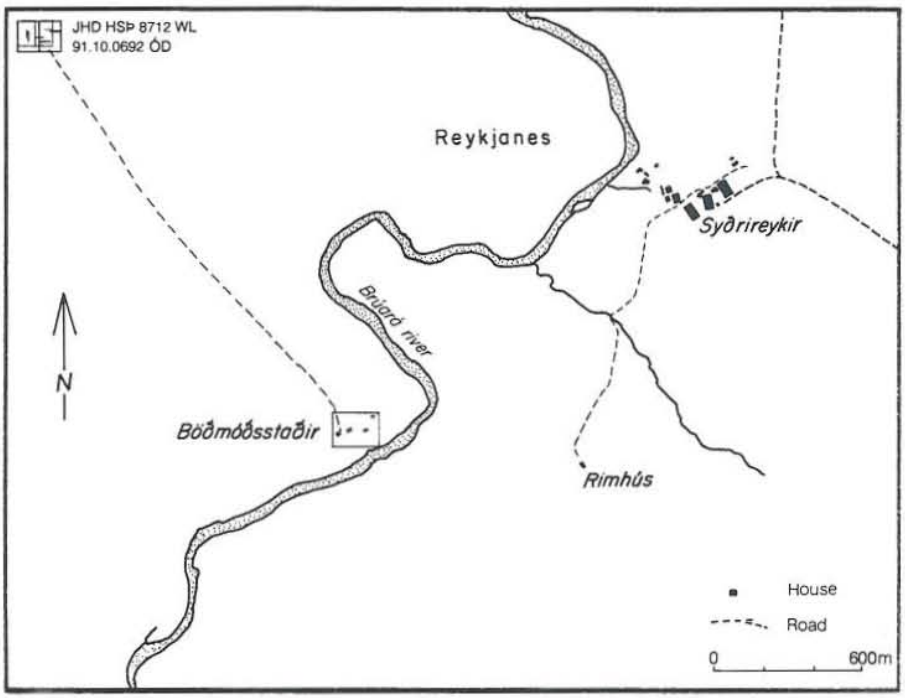

FIGURE 2: The Bodmodsstadir geothermal field and surroundings

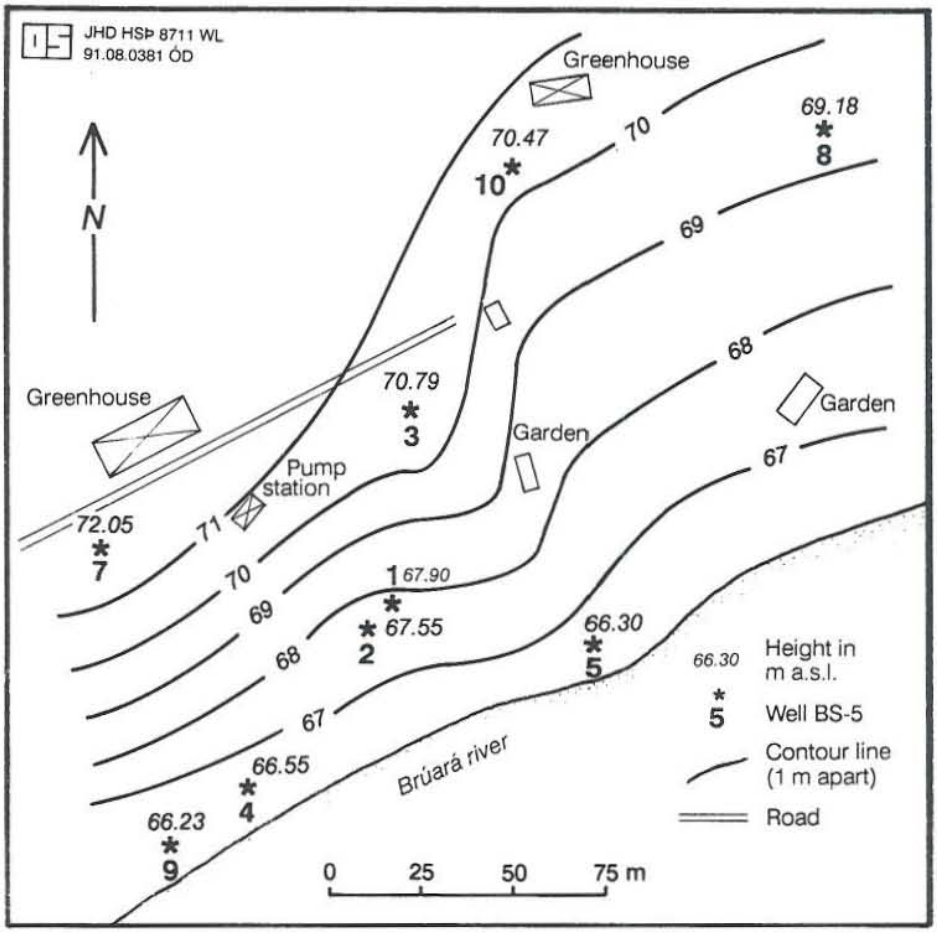

FIGURE 3: Topography and borehole sites at the Bodmodsstadir geothermal field

lithological section of the two deepest boreholes consists mainly of different kinds of basaltic rocks, such as fresh basalt, altered basalt, basaltic breccia and tuff or hyaloclastites below the till and alluvium. An outcrop of the formation to the east of Bodmodsstadir consists of basic and intermediate lavas and/or hyaloclastites, formed during Pleistocene (0.7 m.y. to 3.1 m.y. ago). West of Bodmodsstadir the stratigraphy is younger than 0.7 m.y., but it consists also of lavas and hyaloclastites. The map shows a lot of faults and fractures distributed near the Bodmodsstadir region striking NE. These faults and fractures are the cause of the convective geothermal systems.

There are several hot springs in this area (Figure 4), which discharge about 2 l/s (Olafsson, 1967). Two of the hot springs north of well BS-1 (Figure 4) were manmade, i.e., 1-2 m deep holes were dug and the water taken from them. These holes collapsed after the production in well BS-1 started. The flow from the others has not changed since production started.

2.2 Distribution of soil temperature and low resistivity at depth

Measurements of soil temperature and resistivity sounding have proved to be valuable geophysical methods in prospecting for geothermal resources in Iceland. Measurements of temperature at 0.5 m depth in the soil around hot springs can give important structural information (Flovenz, 1985). Such measurements were performed in June 1990 at Bodmodsstadir (Figure 4). The southern part of the Bodmodsstadir area is characterized by a high surface temperature anomaly of more than 20°C. Wells BS-2, BS-4 and BS-9 are situated in this anomalous area, and most of the hot springs are inside it (Olafsson, 1967). The second high temperature anomaly is located between wells BS-10 and BS-8. The areas with high temperature anomalies lie on a line striking northeast and could be related to a fault or fracture trending in this direction.

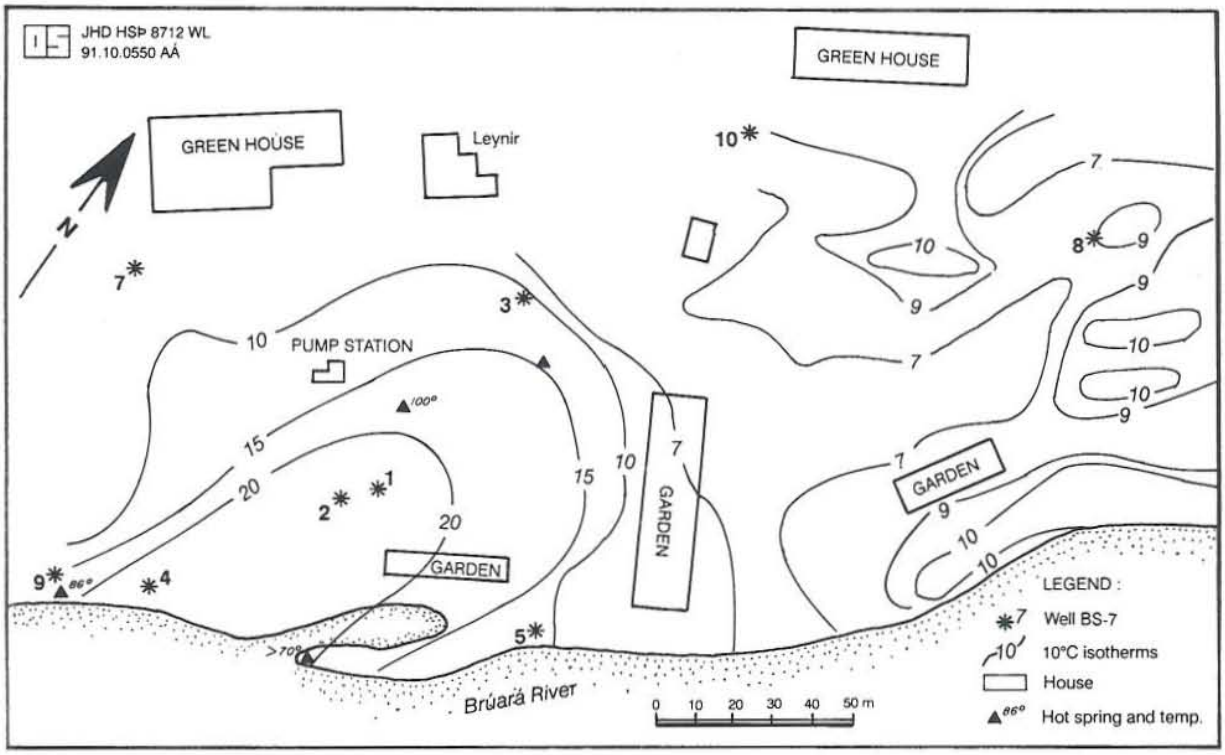

FIGURE 4: Distribution of soil temperature

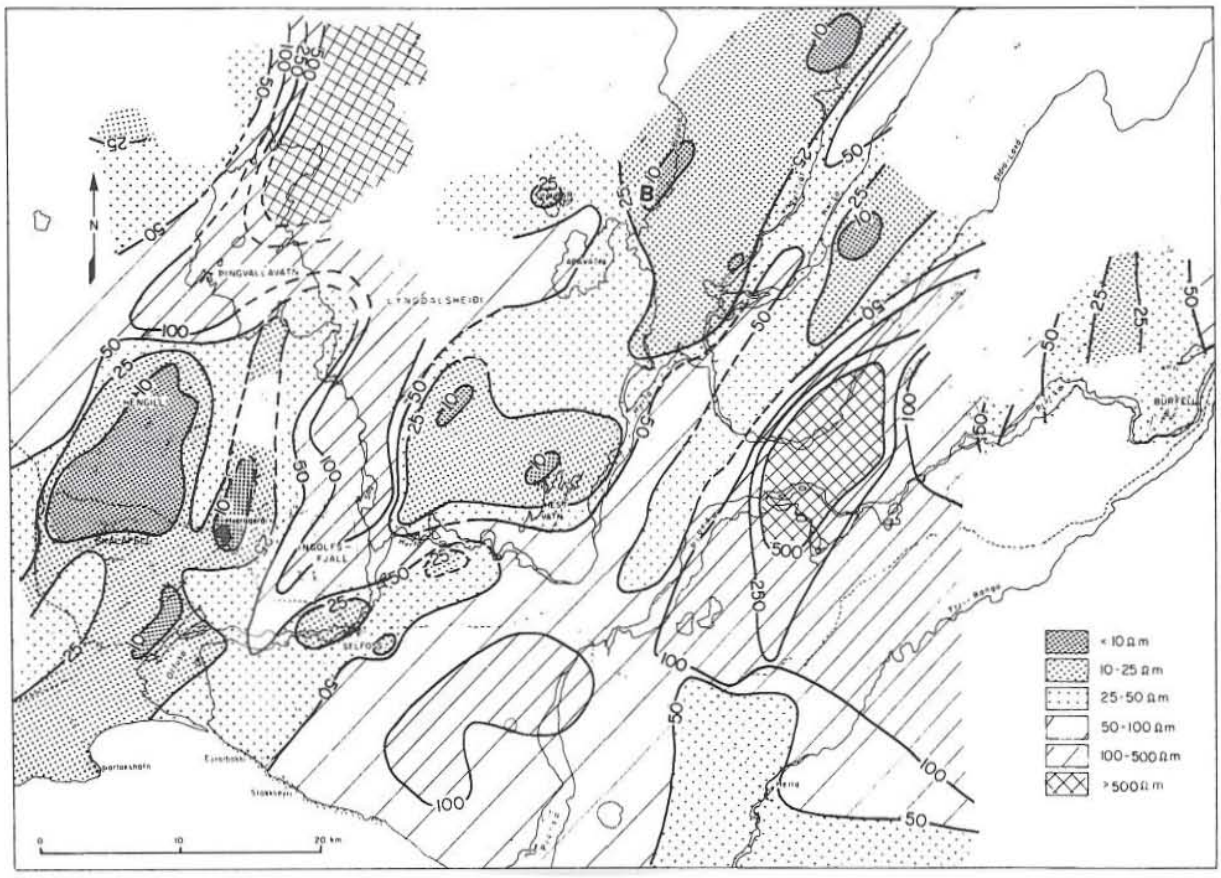

FIGURE 5: Resistivity map of south Iceland at 500 m depth below sea level (from Flovenz et al., 1985); B shows location of Bodmodsstadir

Regional resistivity sounding in southern Iceland has revealed that a low-resistivity anomaly (less than 10 Ωm) exists at 500 m depth around Bodmodsstadir (Figure 5, Bodmodsstadir is shown with the letter B). This anomalous area is characterized by a northeastern strike. Flovenz et al. (1985) concluded that the low-resistivity anomalies were usually caused by intensive geothermal activity. Consequently, surface geothermal activity in the Bodmodsstadir field may be related by a near-vertical fault or fracture to a deeper geothermal system existing below 500 m depth.

2.3 Drilling and production

Since 1974, 10 wells have been drilled at the Bodmodsstadir area. The locations of these wells are shown in Figures 3 and 4, and Table 1 lists their main characteristics. Well BS-6 is located about 300 m north of well BS-7 and is not shown on Figure 4. Wells BS-1 and BS-2 were drilled in 1974 near a hot spring (Figure 4). Well BS-1 has been producing about 10 l/s of boiling water for local greenhouse and space heating since 1974. Eight wells (BS-3 to BS-10) were drilled in May and June 1991. The depths of wells BS-2 and BS-10 are 608 m and 480 m, respectively. The others are very shallow, in the depth range of 48 - 80 m.

More than three temperature logs have been performed in all of the boreholes except in well BS-1 which has been producing since 1974 and in well 6 which has collapsed. The last temperature logs and water level measurements were made on 31 July 1991 for this project. The dates of the temperature logs and water level measured are listed in Table 2. These data, especially the temperature logs, provide the basis for the analysis and simulations below.

TABLE 1: Main characteristics of the wells at Bodmodsstadir

Well no.	x (m)	y (m)	Height (m a.s.l.)	Depth (m)	Casing width (")	Casing length (m)
1	624145.85	414188.52	67.90	38.1	$10\,^{3}/_{4}$	6.3
2	624152.16	414181.27	67.55	610.3	$9\,^{7}/_{8}$	52.9
3	624139.62	414241.81	70.79	80	14	5.8
4	624185.21	414137.59	66.55	49.7	$10\,^{3}/_{4}$	6.5
5	624091.36	414177.42	66.30	74.5	$10\,^{3}/_{4}$	6.5
6	624497.56	414530.42	76.76	67.5	$10\,^{3}/_{4}$	6.5
7	624224.75	414202.97	72.05	49.5	plastic casing	25(?)
8	624026.82	414318.17	69.18	49.5	$7\,^{5}/_{8}$	5.9
9	624206.59	414122.12	66.23	49.5	$10\,^{3}/_{4}$	7.0
10	624111.31	414307.93	70.47	482.8	$10\,^{3}/_{4}$	11.0
					$8\,^{5}/_{8}$	70.2

TABLE 2: Temperature logging and water level at Bodmodsstadir

Well no.	Drilling dates (from...to..)	Temperature logging dates	Water level* (m a.s.l.)
1	31-07-74- 08-08-74		
2	10-08-74- 28-08-74	24-10-74 31-08-89 31-07-91	71.25*
3	13-05-91- 15-05-91	14-05-91 14-05-91 15-05-91 15-05-91 31-07-91	66.74
4	15-05-91- 16-05-91	16-05-91 22-05-91 31-07-91	66.35
5	16-05-91- 22-05-91	17-05-91 21-05-91 22-05-91 28-05-91 31-07-91	65.68
6	17-05-91- 21-05-91	21-05-91	
7	21-05-91- 22-05-91	22-05-91 23-05-91 31-07-91	67.3
8	22-05-91- 23-05-91	23-05-91 24-05-91 27-05-91 28-05-91 31-07-91	66.28
9	24-05-91- 27-05-91	27-05-91 28-05-91 31-07-91	66.01
10	27-05-91- 07-06-91	27-05-91 28-05-91 29-05-91 31-05-91 05-06-91 10-06-91 15-06-91 29-06-91 31-07-91	72.47

* water level measured on 31 July 1991.
⋆ measured on 1 October 1991.

3. TEMPERATURE DISTRIBUTION AND CONCEPTUAL MODEL

From the temperature log data and water level measurements as well as the geological structure, an attempt is made below to determine the locations of aquifers, the direction of flow in the formation, the formation temperature and to establish a conceptual model of the Bodmodsstadir geothermal field. All the aquifers found in the boreholes are very small except in well BS-1 which is used for production.

3.1 Interpretation of temperature logs and locations of aquifers

Well BS-1: Well BS-1 was completed in August 1974. No temperature logs have been performed in this well because it has been producing since it was drilled (self-flowing).

Well BS-2: Well BS-2 was completed in August 1974, and was cased down to 52.9 m depth. The first temperature measurement in well BS-2 was performed two months later (Figure 6A). Recent temperature measurements were performed in August 1989 and in July 1991. The temperature curve measured in 1991 is almost the same as that measured in 1989, and since there are no signs of internal flow in the well the temperature profile obtained in 1991 represents the formation temperature in the well. The temperature curves show a 96°C hot aquifer behind the casing at 20-30 m depth. Drilling reports mention several possible aquifers at depths of about 190 m, 306 m, 340 m, 363 m and 543 m (State Drilling Contractors, 1974). This is based on changes in water level during drilling and/or on drilling speed. For example, when the borehole was 135 m deep, the water level was at 0.9 m depth, but when it was 230 m, the water table was at zero, so there must be an aquifer in this interval. The drill cuttings show a petrological change from basaltic breccia to altered basalt at 190 m depth, but the temperature measurements show no indications about this aquifer. The temperature curve obtained in 1974 gives information about the deeper aquifers. At about 300 m depth, the temperature gradient increases, indicating an aquifer there. Between 350 m and 370 m depth, the temperature does not change, i.e., there is an internal flow in the well between two aquifers. At 400 m and 550 m depth the gradient changes, probably because of aquifers at these depths.

Well BS-3: Well BS-3 was completed on May 15, 1991. The temperature curves obtained during drilling (Figure 6B) show an aquifer at 23-24 m depth. All the temperature measurements indicate another aquifer at about 35 m depth but the measurements after drilling show a change in the gradient at this depth. The great cooling at the bottom in the two measurements during drilling also suggest an aquifer there. There is also a possible aquifer close to the bottom of the well or at about 75 m depth.

Well BS-4: Well BS-4 is very close to well BS-2 and was completed on May 16, 1991. As in well BS-2 there is a maximum in temperature (Figure 6C) at about 25 m depth showing a horizontal flow in the vicinity of the well. During drilling, 80-90°C water entered the well at about 20 m depth indicating an aquifer there.

Well BS-5: Well BS-5 was completed on May 22, 1991. Five temperature logs have been performed in this well (Figure 6D). The temperature measurements do not show any clear signs of aquifers in the well and the drilling report recorded almost no water in the well during drilling (Icelandic Drilling Company, 1991), so there are no major aquifers in this well. When the last temperature measurement was performed (07-31-1991) the well had probably recovered after drilling and, therefore, it shows the formation temperature around the well.

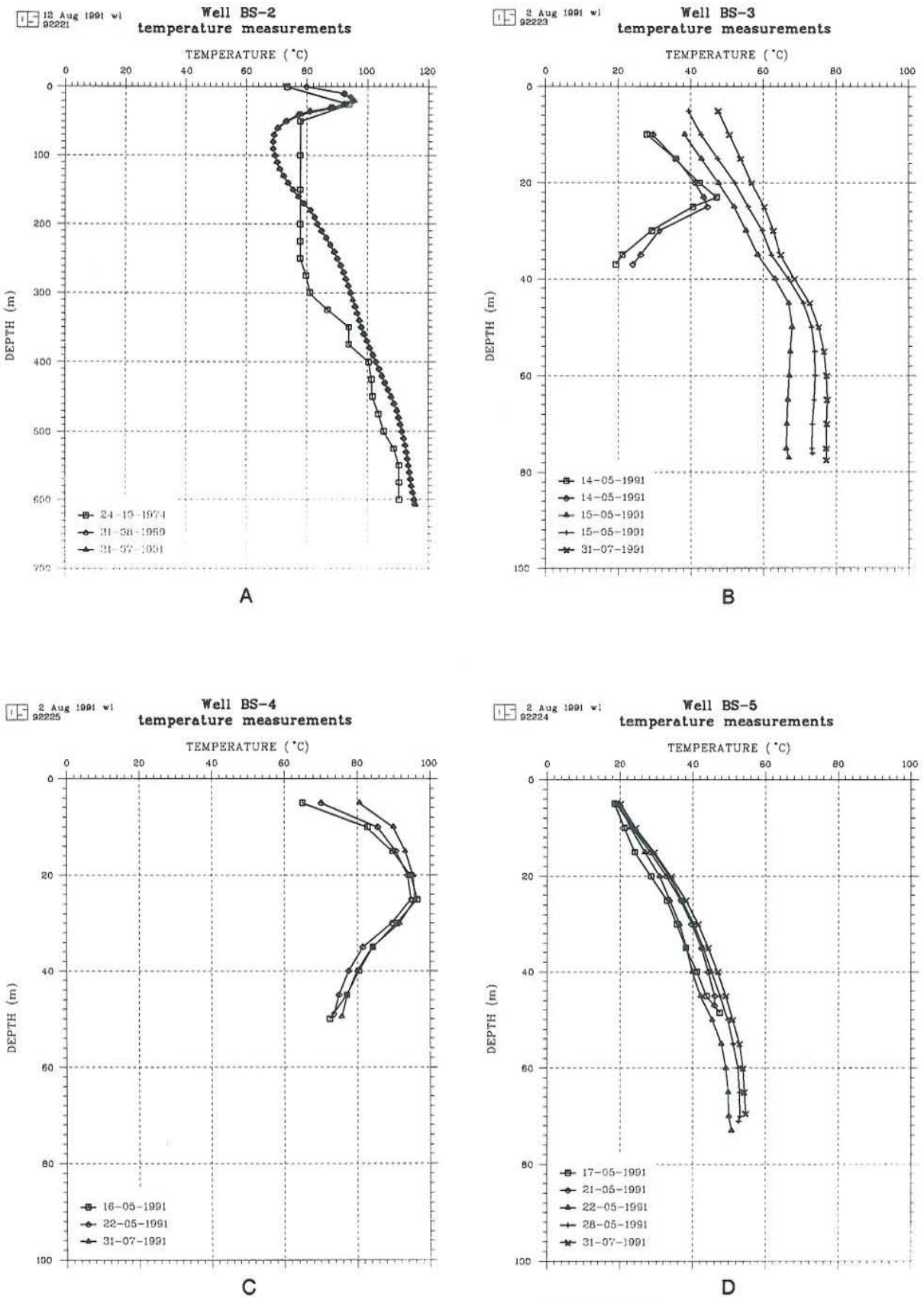

FIGURE 6: Temperature measurements in wells BS-2, BS-3, BS-4 and BS-5

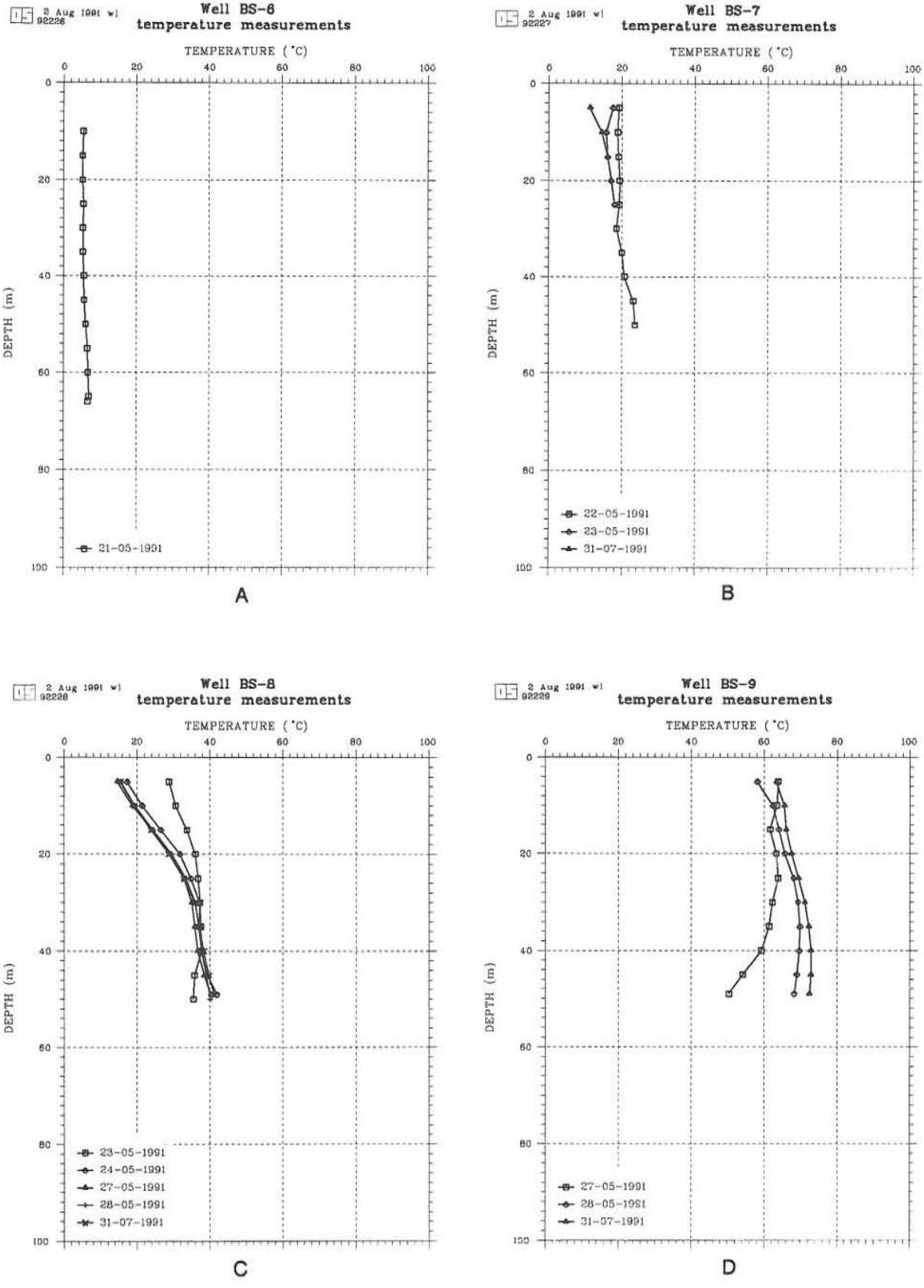

FIGURE 7: Temperature measurements in wells BS-6, BS-7, BS-8 and BS-9

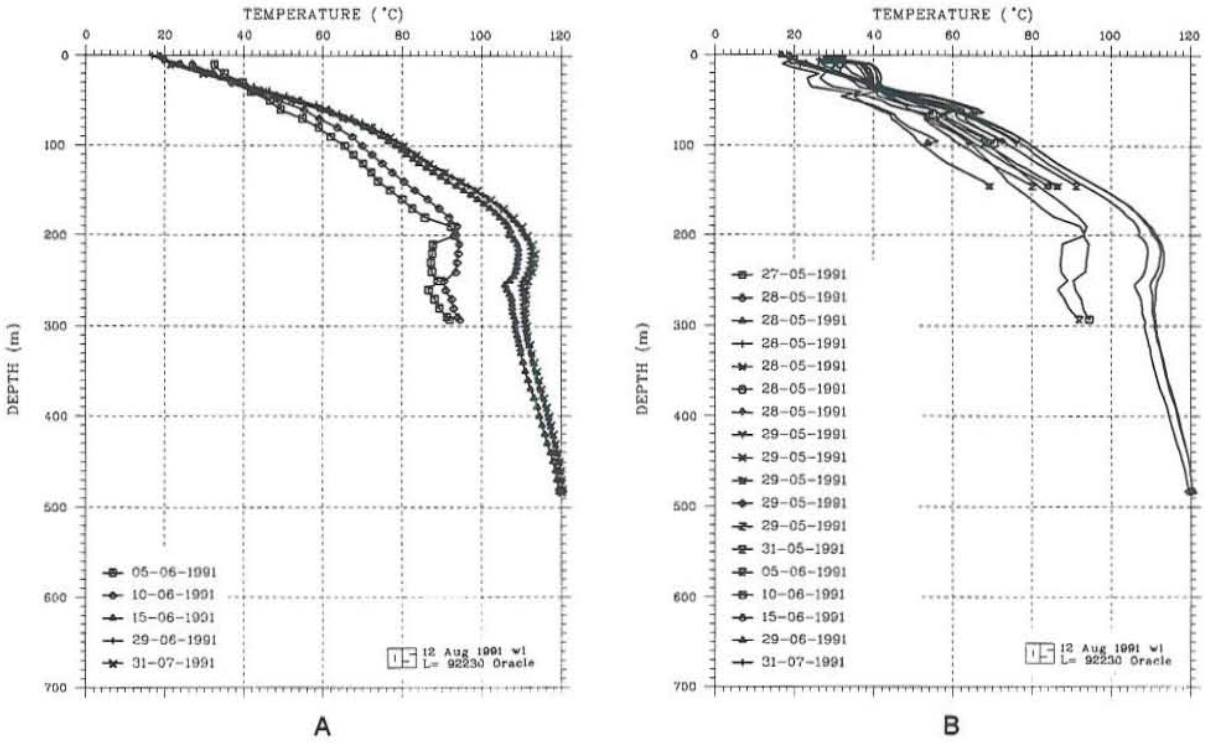

FIGURE 8: Temperature measurements in well BS-10

Well BS-6: Well BS-6 was completed on May 21, 1991 at 67.5 m depth, but it collapsed at 6 m depth soon after drilling. Temperature data from May 21, 1991 after the well was completed show that cold water flows into the well at shallow depth (Figure 7A). The drilling report shows a small aquifer at 24-25 m depth with cold water and a few smaller aquifers deeper (Icelandic Drilling Company, 1991). This well is about 300 m north of the next well and obviously outside the hot reservoir.

Well BS-7: Well BS-7 was completed on May 22, 1991 at 49.5 m depth but it also collapsed soon after drilling at 25 m depth. Temperature curves (Figure 7B) reflect that cold water of about 20°C enters this borehole. The drilling report recorded two aquifers at 24-25 m and 30-40 m depths, both cold (Icelandic Drilling Company, 1991).

Well BS-8: Well BS-8 was completed on May 23, 1991, after which time five temperature measurements have been performed (Figure 7C). An aquifer at 42-43 m depth can be seen on the first temperature measurement. The drilling report recorded water inflow at 42-43 m depth (Icelandic Drilling Company, 1991).

Well BS-9: Well BS-9 is very close to well BS-4. It was completed on May 27, 1991. Three temperature measurements have been performed in the well after that time (Figure 7D). All the measurements show temperature reversal indicating hot horizontal flow at about 40 m depth. No aquifer can be seen on the temperature measurements, but a few small aquifers are mentioned in the drilling report (Icelandic Drilling Company, 1991).

Well BS-10: Well BS-10 was completed in June 1991 at 482.8 m depth. During and after drilling, many temperature measurements were made (Figure 8A and 8B). There is no difference between the temperature curves measured on June 29 and July 31, 1991 and no signs of internal flow which means that the last temperature measurement represents the formation temperature. Four

aquifers located at 20 m, 60 m, 195 m, and 250 m can be seen on the temperature curves in Figure 6A.

The locations and temperatures (if known) of the minor aquifers in the Bodmodsstadir wells are listed in Table 3. To establish a conceptual model of a geothermal field, it is very important to determine the regional features of the flow and to compare them with the aquifers in the wells. At Bodmodsstadir, we are mainly interested in the distribution of aquifers with temperature around 100°C. It is likely that the 95°C shallow aquifers in wells BS-2, BS-4 and BS-9 are connected to the aquifer at 215-240 m depth in well BS-10.

TABLE 3: Location and temperature of aquifers in BS-2, BS-3, BS-4, BS-5, BS-7, BS-8, BS-9 and BS-10

Well no.	Depth (m)	Temperature (°C)
1		location of aquifers not known...
2	20-30 190 306 350 370 400 550	96 (horizontal flow) 80 >94 (?) 100 110
3	23-24 35 75	>44 62 78
4	25	95 (horizontal flow)
5		no aquifers
6		collapsed
7	24-25 30-40	cold water cold water
8	42-43	
9	30-40	72 (horizontal flow)
10	20-30 60 195 250	42

3.2 Formation temperature and temperature profiles

Since there is very little temperature difference between the two latest measurements in the wells, it is reasonable to assume that the temperatures measured in each well on 31 July 1991 represent the formation temperature around the wells (Figure 9). There is a considerable lateral change in temperature at shallow depths between the wells. Below 100 m depth, the formation temperature in well BS-10 is much higher than that in well BS-2. Based on this data, the temperature distributions in two cross-sections and at three different depths were constructed (Figures 10, 11, 12, 13 and 14).

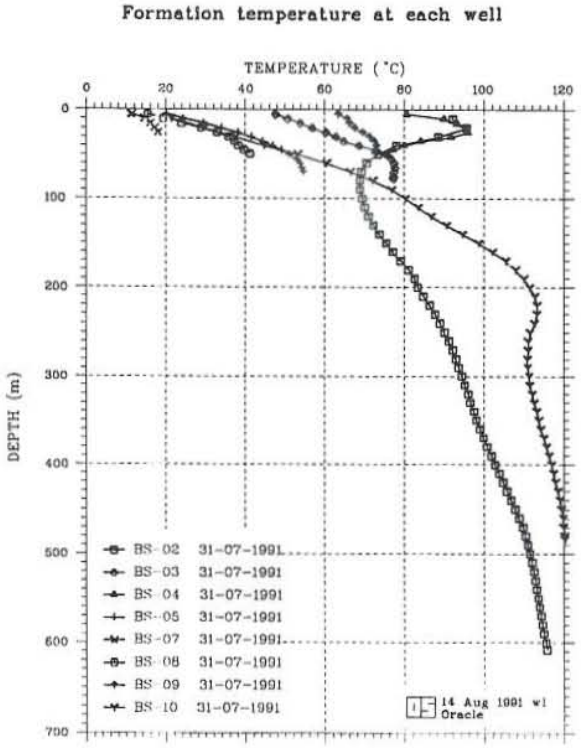

Figure 10 represents the temperature cross-section from well BS-9 to well BS-8. The temperature distribution is characterized by a high temperature anomaly (over 90°C) beneath wells BS-4 and BS-2. This is caused by a horizontal flow of hot water perpendicular to the cross-section. The shape of the temperature distribution below 100 m depth shows an upflow between wells BS-2 and BS-10, much closer to well BS-10 at depth. Figure 11 shows the temperature cross-section from well BS-7 to well BS-5. It can be seen on this cross-section that the hot water flows horizontally perpendicular to this cross-section. It can, therefore, be said that the temperature distribution is controlled by a convective flow of hot water.

FIGURE 9: Formation temperature in eight wells at Bodmodsstadir

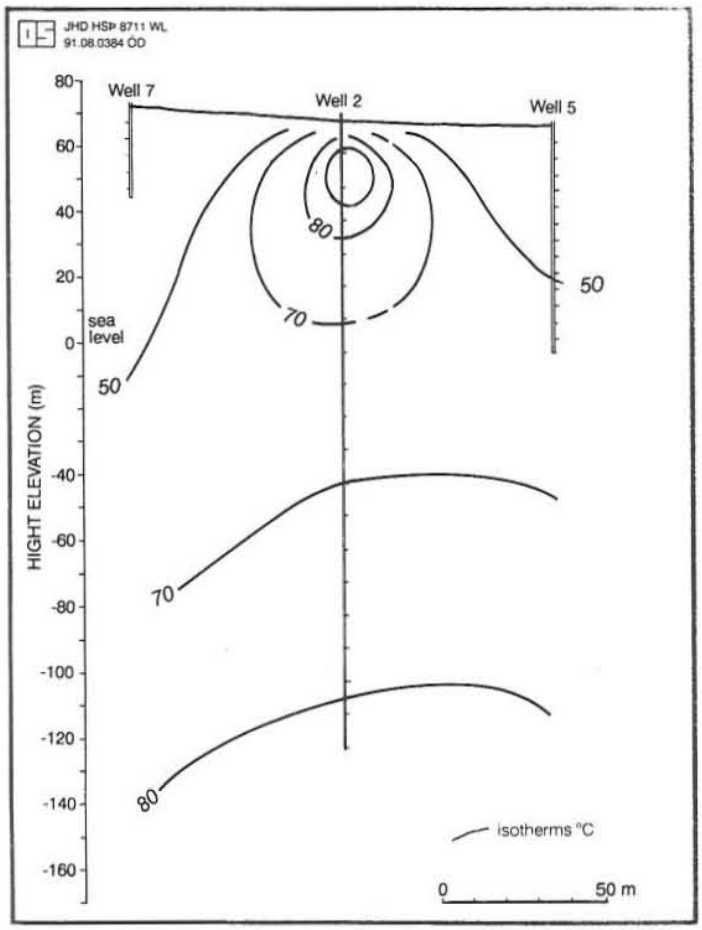

FIGURE 11: Temperature cross-section between wells BS-7 and BS-5

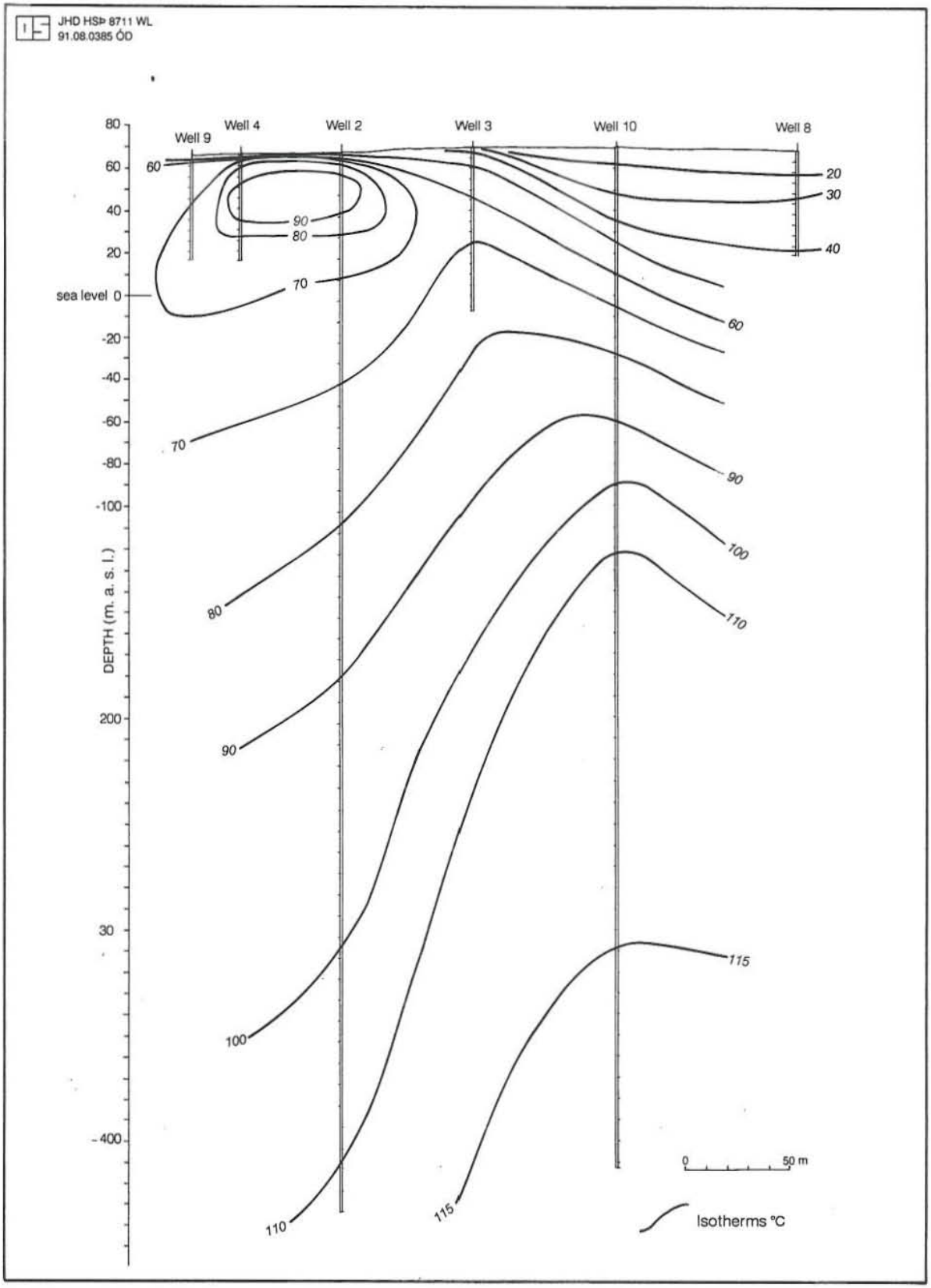

FIGURE 10: Temperature cross-section between wells BS-9 and BS-8

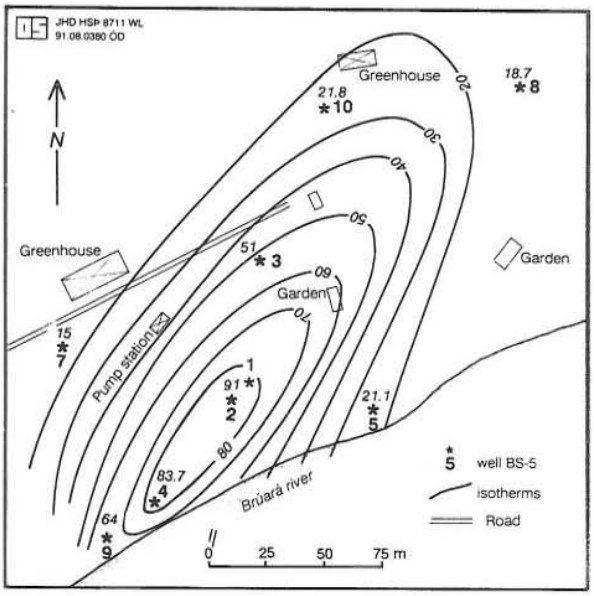

FIGURE 12: Temperature distribution at 60 m (a.s.l.)

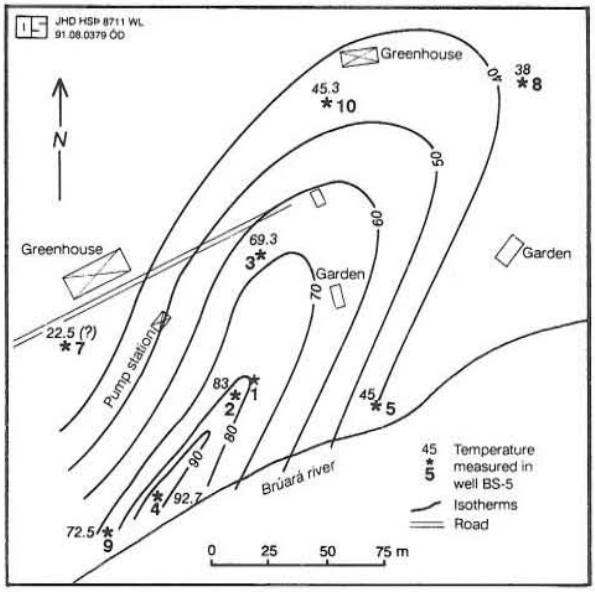

FIGURE 13: Temperature distribution at 30 m (a.s.l.)

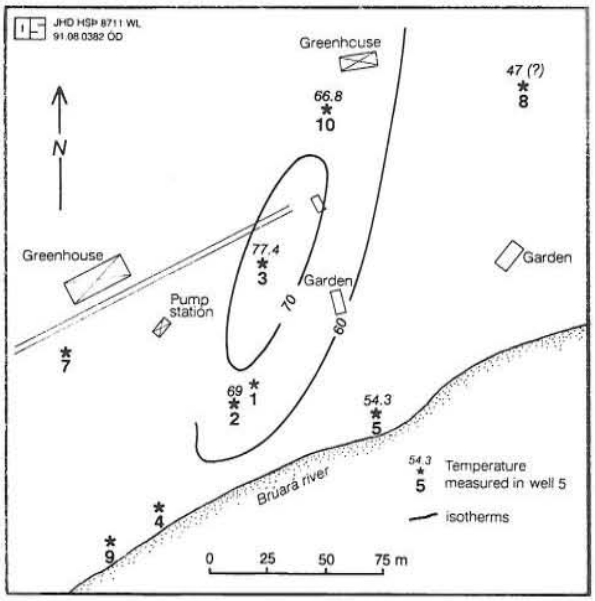

FIGURE 14: Temperature distribution at sea level

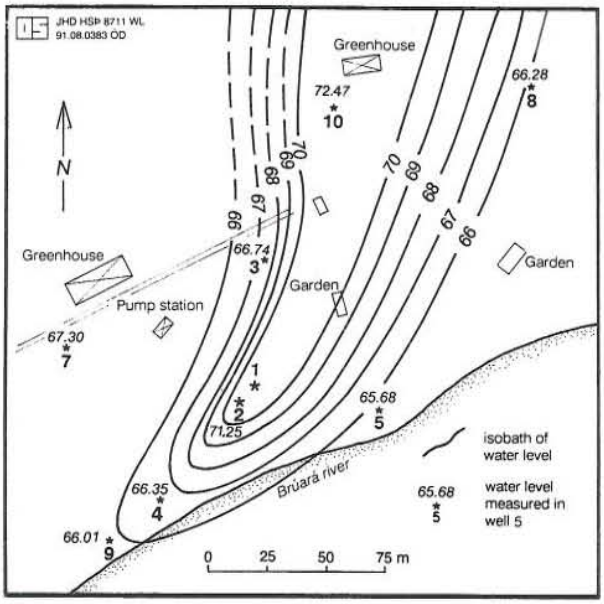

FIGURE 15: Water level at Bodmodsstadir in m a.s.l.

3.3 Temperature distribution at different depths

Based on the formation temperature in each well, temperature distributions at different depths were constructed and are plotted in Figures 12, 13 and 14. A high temperature anomaly can be seen on all the figures. For example, at 60 m and 30 m depth (a.s.l.), the high temperature anomalies are located in the southern part, including wells BS-2 and BS-4. At sea level the anomaly has moved in a NE direction and now includes well BS-3, but wells BS-2 and BS-4 are outside the high temperature anomaly. All temperature anomalies at different depths are

dominantly striking N40°E, supporting the theory of a fracture, perhaps a fault, located between wells BS-2 and BS-10 striking in this direction with hot water flowing along it.

3.4 Water level and pressure

The water level in the wells reflects the reservoir pressure. The differences in water level can give important information on the flow direction in the reservoir. The water levels in most of the wells were measured on 31 July 1991 (Table 2) and are plotted in Figure 15. As can be seen from Figure 15, the water level is highest in well BS-10, indicating a higher reservoir pressure there.The shape of the water level surface indicates a flow from well BS-10 to well BS-2 probably from a fault that is located between these wells striking NE.

Figure 16 shows water level measurements in well BS-10 during the first 50 days after it was completed. The water level rose rapidly for the first 2-3 days, or about 8 m, then it levelled out and rose another 4 m for the rest of the time interval. Hot water flows into the well at about 220 m depth and warms it up, the water column becomes lighter and the water level rises.

Using the formation temperature and water level in wells BS-2 and BS-10, the pressure profile in the wells (Figure 17) were calculated using the program PREDYP (the wellhead of BS-10 is set at zero depth). Below 300 m, the pressure in the two wells is almost the same. But it is slightly higher in well BS-10 than in well BS-2 above 300 m depth. This indicates that hot water may flow in the direction from well BS-10 to well BS-2.

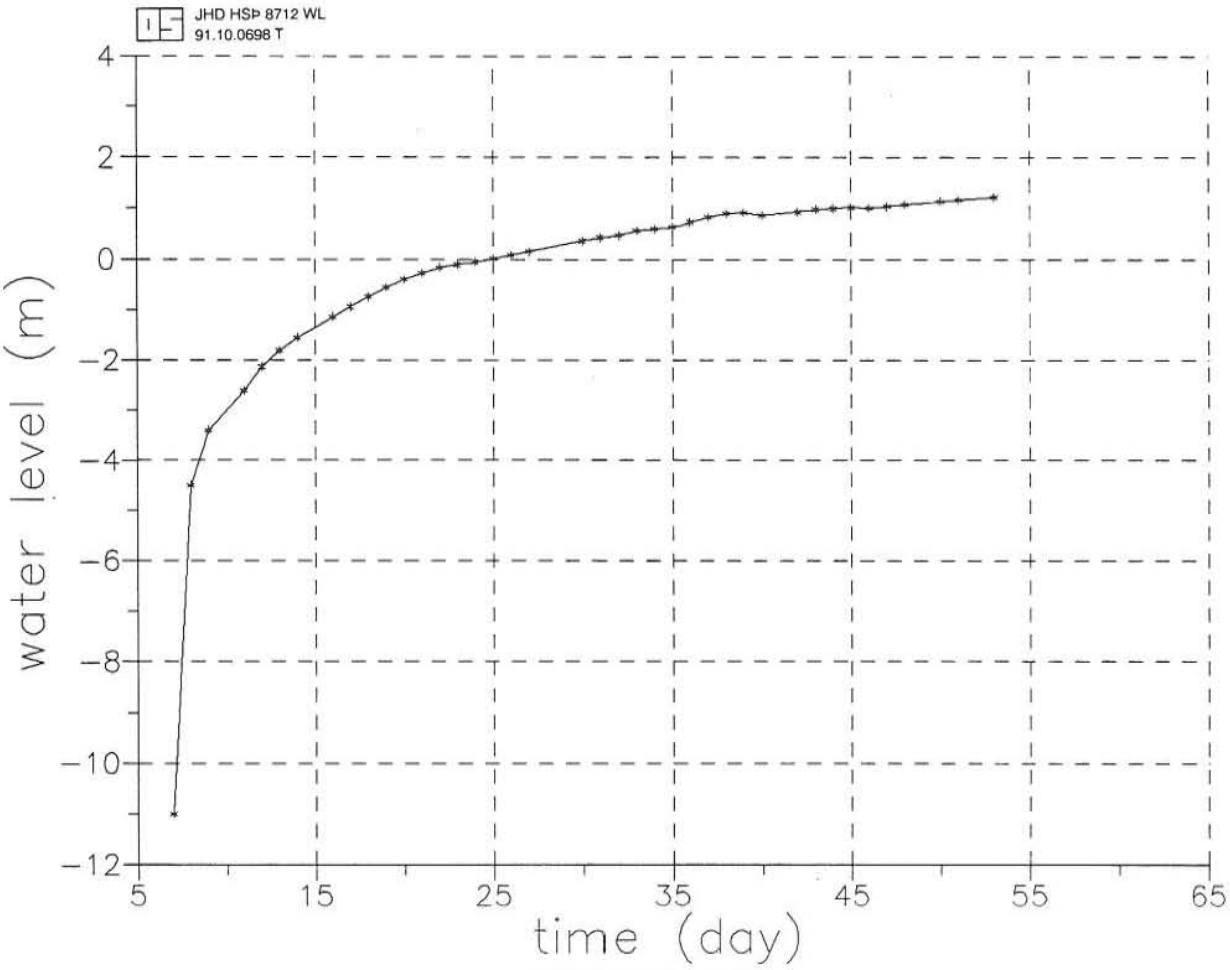

FIGURE 16: Water level versus time in well BS-10

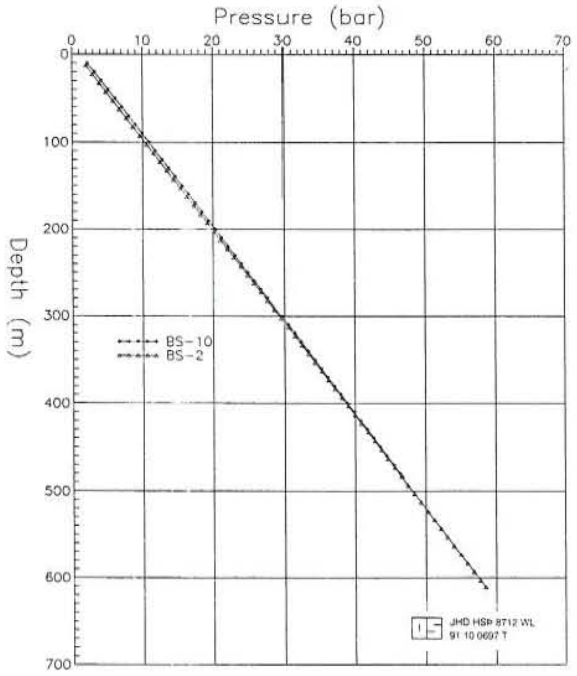

FIGURE 17: The pressure profile of wells BS-2 and BS-10

3.5 Conceptual model of the Bodmodsstadir geothermal field

The general characters of the Bodmodsstadir geothermal field are summarized below:

1. There is an anomaly in the soil temperature striking NE.

2. Many faults and/or fractures chiefly striking NE were found by surface geological investigation west and east of Bodmodsstadir. Low-resistivity anomalies were revealed at 500 - 600 m depth beneath this area.

3. Distribution of the formation temperature measured in eight wells is intensively affected by convection of hot water. A horizontal flow exists at 30 - 60 m depth, and a vertical upflow exists between wells BS-2 and BS-10 below 100 m depth.

4. The water level surface in the area and the pressure in wells BS-2 and BS-10 show that the flow direction is from NE to SW.

5. The distribution in the formation temperature at different depths also shows that the direction of the hot flow is NE.

All of these features can be explained by supposing a permeable fracture or fault striking NE and slightly dipping to the west, located between wells BS-2 and BS-10 with hot water flowing vertically along it up to about 30 m depth near well BS-10, then flowing horizontally towards wells BS-4 and BS-9.

A conceptual model of the Bodmodsstadir geothermal field has been established (Figure 18). This model consists of the supposed NE striking fracture and two horizontal aquifers at 30 m and 230 m depth. The arrows in Figure 18 represent the flow direction. This model will be calibrated using the steady-state and the non-steady-state simulations in the next two chapters.

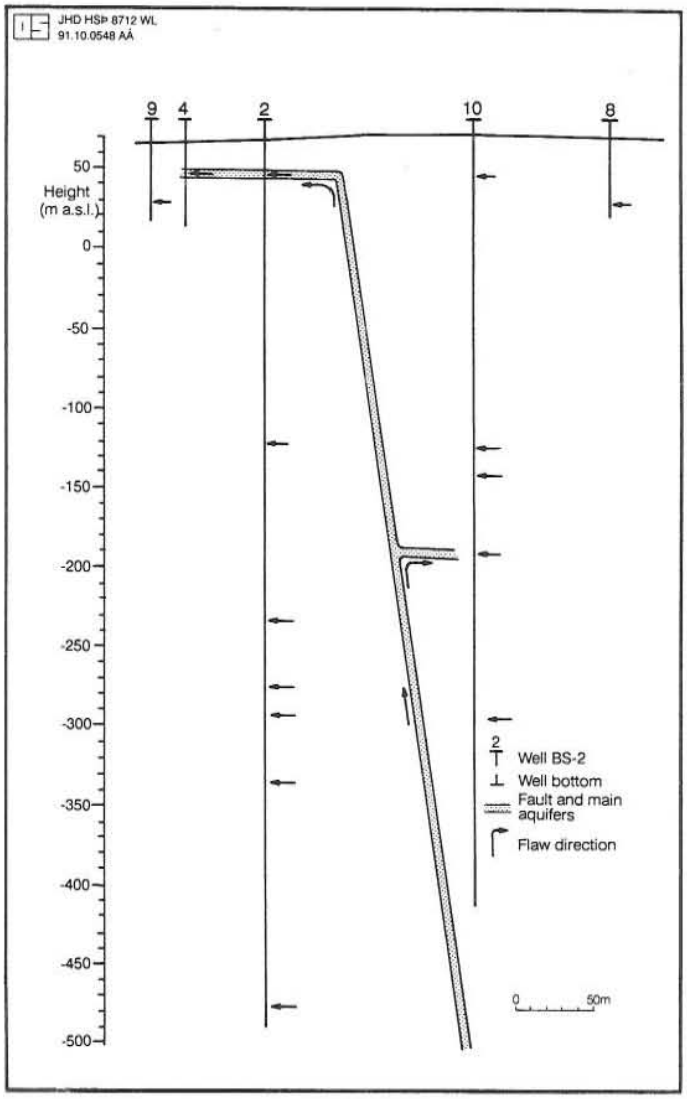

FIGURE 18: A conceptual model of the Bodmodsstadir geothermal field

4. STEADY-STATE SIMULATIONS OF THE TEMPERATURE DISTRIBUTION

The conceptual model, established in the former chapter, is characterized by a supposed fracture trending close to N40°E and two horizontal aquifers. In order to examine the possible direction and natural state of the fracture at depth, the VARMI program is employed to simulate the temperature distribution in two dimensions under steady-state conditions. Temperature distributions in two profiles, which intersect perpendicularly, are simulated with different initial models, and are compared with formation temperature obtained from temperature logging. In the simulation, conditions at open boundaries, including the fracture dip and the temperature of the upflow, are gradually changed until the calculated temperature distribution fits the formation temperature satisfactorily. The final model can be used to put some constraints on the possible location of the main aquifers in the Bodmodsstadir geothermal field. It will also be used to construct the initial model for the PT program, which takes time dependency into account.

4.1 Steady-state simulation – the VARMI program

Temperature distribution in a steady-state condition obeys the Laplace equation. In two dimensional space with homogeneous isotropy medium, the Laplace equation can be written as:

$$\frac{\partial^2 T}{\partial x^2} + \frac{\partial^2 T}{\partial z^2} = 0 \qquad (1)$$

The VARMI program solves this equation numerically by using a finite element method. Two types of boundaries, open boundaries and closed boundaries, are defined in this program. Fractures and aquifers within two-dimensional space can be treated as line sources (or open boundaries), and the edges of the space can be regarded as closed boundaries. In the calculations, the temperature is fixed, both at the open and the closed boundaries according to available data and assumptions of the temperature within the aquifers and the undisturbed regional temperature gradient.

A grid consisting of triangle blocks is needed to run the program VARMI. The triangles are kept small in the area where the highest accuracy in the calculations is required and where the highest temperature gradients are expected. Before the actual simulations, the initial grid can be automatically refined. The output from VARMI includes the temperature at each triangle node and plots of the spatial temperature distribution in two dimensions. Figure 19 shows an example of an initial grid (Model 1).

4.2 Model 1

The supposed fracture is striking N40°E; a cross-section perpendicular to it is chosen as Model 1. Wells BS-2 and BS-10 are then projected on the cross-section so that the calculated temperature can be compared with the formation temperature measured in the two wells. The fracture is dipping towards well BS-10 with a 6.5° dip angle. Two horizontal aquifers are set at 30 m and 230 m depths (Figure 19). The fracture and the two horizontal aquifers are regarded as 2-dimensional open boundaries. Hot water flows vertically along the fracture.The temperature of the hot water is assumed to be 130°C at 1000 m depth, 116°C at 230 m depth and 95°C at 30 m depth. At 230 m depth, 116°C hot water flows horizontally towards well BS-10. Well BS-10 did not intersect this aquifer but the temperature logs show that such a horizontal flow must be close to the well. A distance of 10 m is assumed between well BS-10 and the aquifer at this depth.

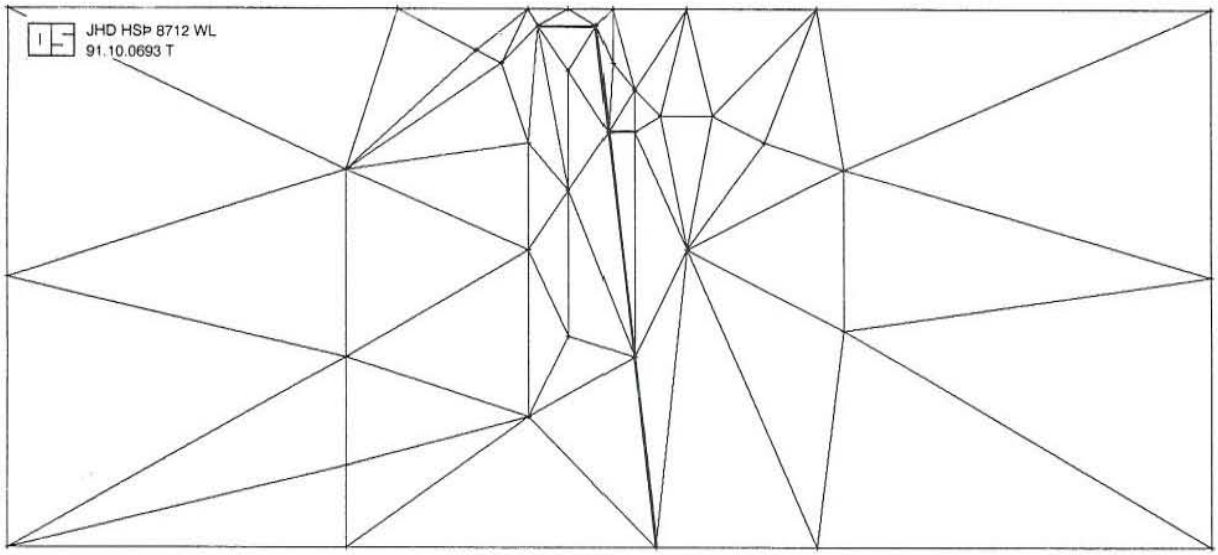

FIGURE 19: Model 1 and initial triangle grid. The thick line represents fracture and aquifers

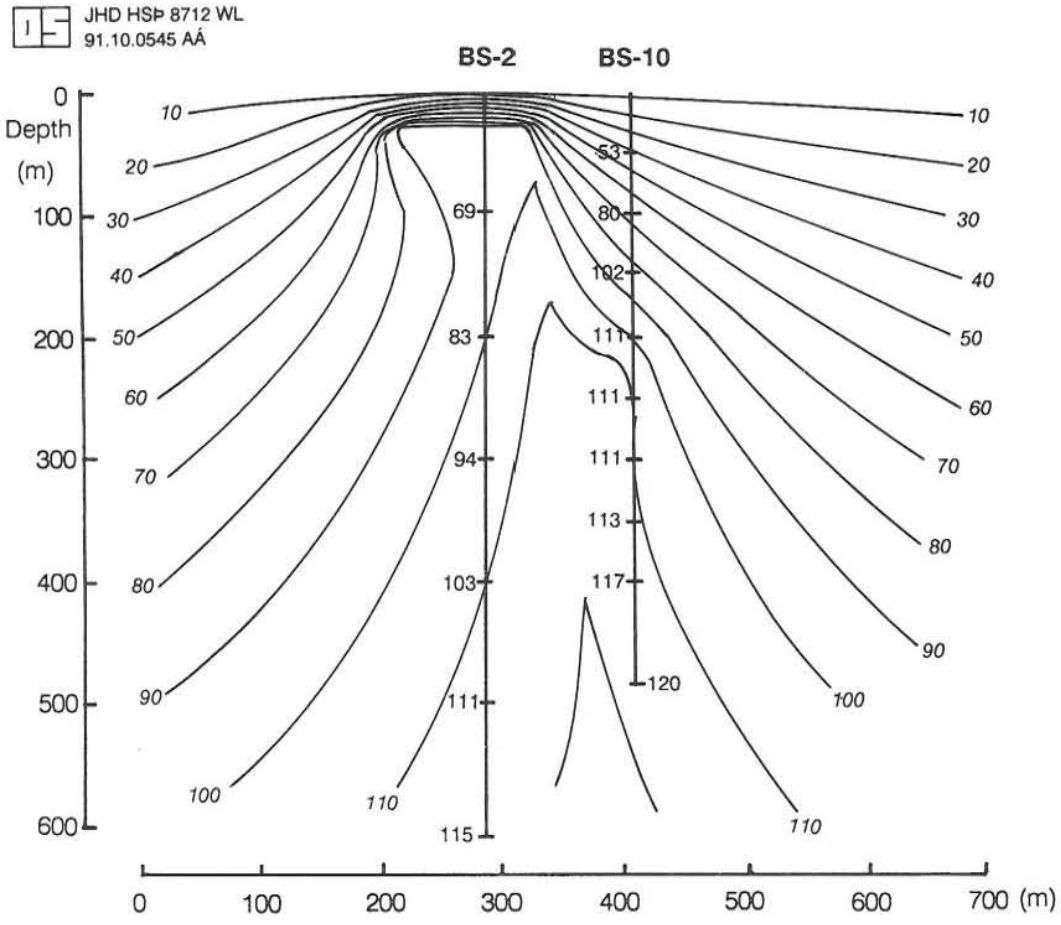

FIGURE 20: Temperature distribution resulting from Model 1

At 30 m depth, 95°C hot water flows horizontally from the fracture to wells BS-1 and BS-2. The aquifer at 30 m depth is perhaps related to the boundaries of the till and alluvium in the Bodmodsstadir area.

Model 1 is 2300 m long and 1000 m deep. The temperature at the surface is set at 4°C which is the annual mean temperature, and 126°C/km regional average temperature gradient is assumed at the left and right boundaries.

Figure 20 shows the temperature distribution using Model 1. Comparison with the formation temperature measured at wells BS-2 and BS-10 shows large temperature differences. The calculated temperatures are higher than the measured temperature from 100 m depth to 500 m depth at well BS-2, and lower in the upper part (above 100 m depth) at well BS-10. For the deeper part of well BS-10 the fit is good, and the temperature reversal in the shallow part at well BS-2 is matched adequately. This suggests that the position and the temperature of the shallow horizontal aquifer is reasonable. A small temperature reversal occurs at about 300 m depth at well BS-10 in Figure 20. This feature is consistent with the formation temperature obtained from temperature logging in well BS-10. In order to get better fit, the positions and temperatures of the aquifers in Model 1 have to be modified.

4.3 Model 2

Model 2 is obtained by changing the conditions at the open boundaries in Model 1. Figure 21 shows the initial triangle grid for Model 2 and Figure 22 presents the temperature cross-section and the comparison between the calculated and measured temperatures at wells BS-2 and BS-10. The calculated temperature distribution matches the measured formation temperature satisfactorily at these wells. Temperature reversal in the upper part of well BS-2 is also closer to the measured formation temperatures.

The dip-angle of the fracture in Model 2 is 7.8° and the fault has been moved 40 m horizontally towards well BS-10 from Model 1. In this case, the horizontal distance from the bottom of well BS-10 to the fracture is only a few meters. The depth of the deep horizontal aquifer is 200 m, 30 m shallower than that in Model 1. The temperature of this aquifer is increased to 118°C. The depth and temperature of the shallow aquifer has not been changed. In Model 2 another horizontal aquifer is set at 70 m depth with 95°C hot horizontal flow towards well BS-10, in order to fit the simulated results with the formation temperature in the upper part of well BS-10.

The simulated result using Model 2 fits well with the measured formation temperature. Model 2 is, therefore, much better than Model 1 and is considered the final result of the steady-state simulation.

4.4 Model 3

Model 3 represents a model perpendicular to Model 2, roughly from well BS-7 to well BS-5. A supposed fracture, the same one as in Model 2, is set close to well BS-2 and it dips towards well BS-7. This fault is the open boundary in Model 3, where hot water flows up. In the vertical aquifer, the temperature is 114°C at 600 m depth and 90°C at 250 m depth. A point source is set near well BS-2 at 30 m depth and with temperature of 95°C. The close boundaries in Model 3 are the same as in Model 1 or Model 2.

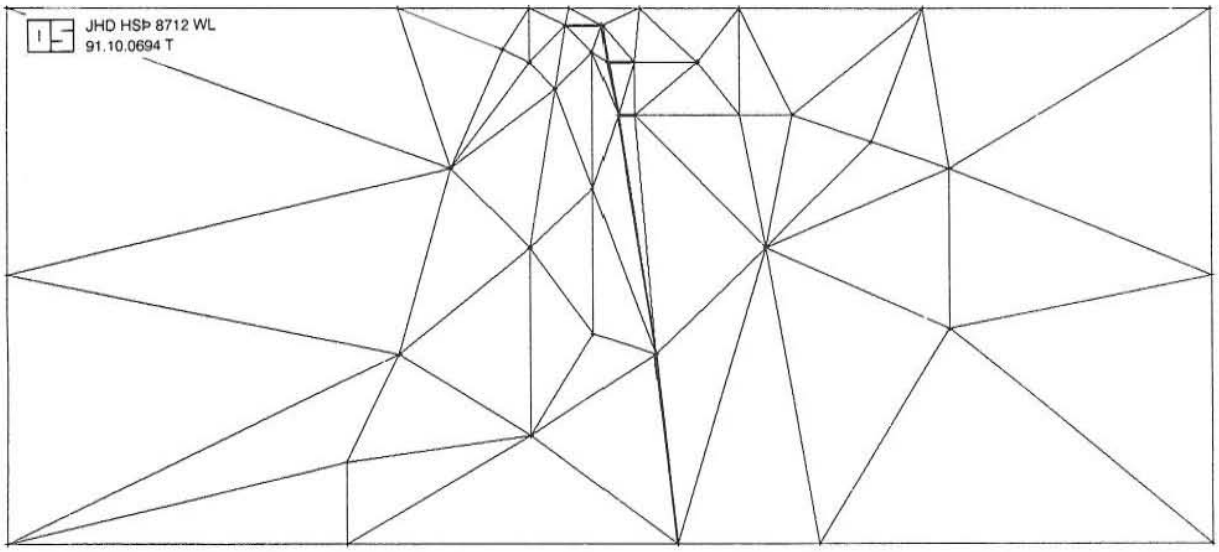

FIGURE 21: Model 2 and initial triangle grid. The thick line represents fracture and aquifers

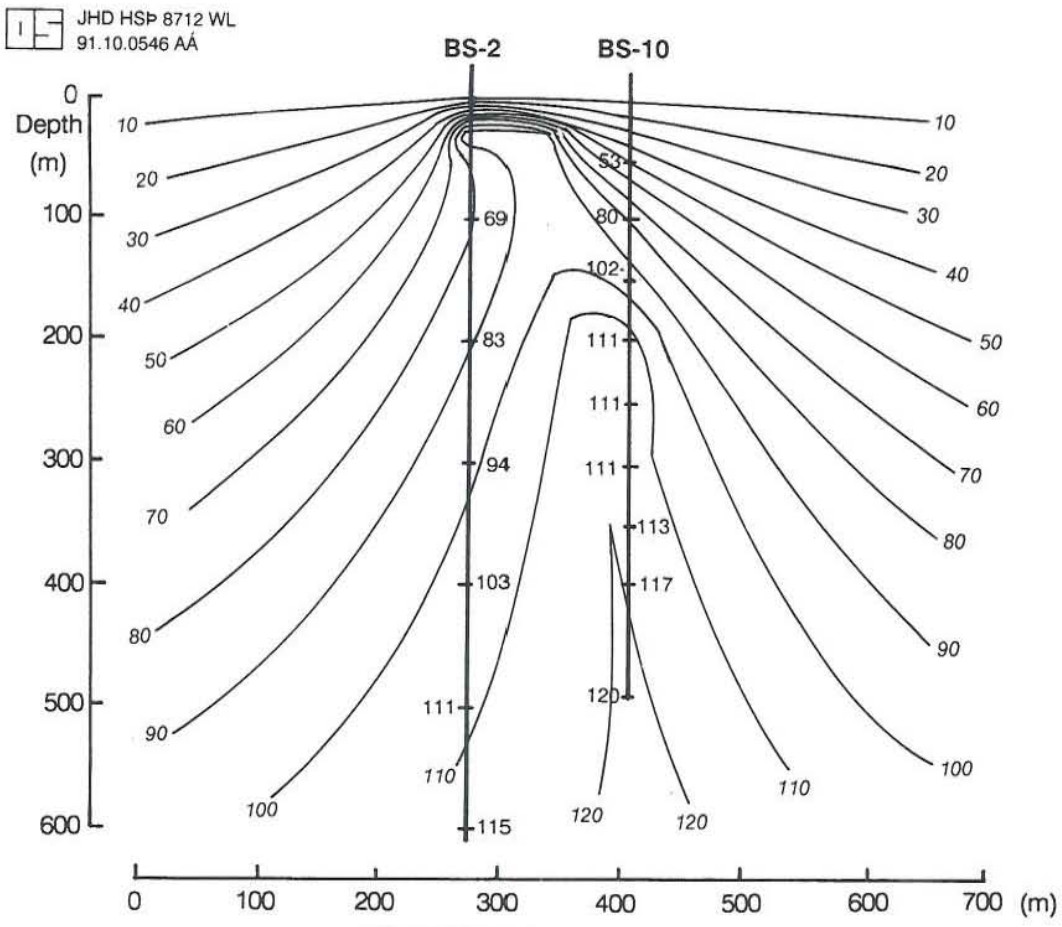

FIGURE 22: Temperature distribution resulting from Model 2

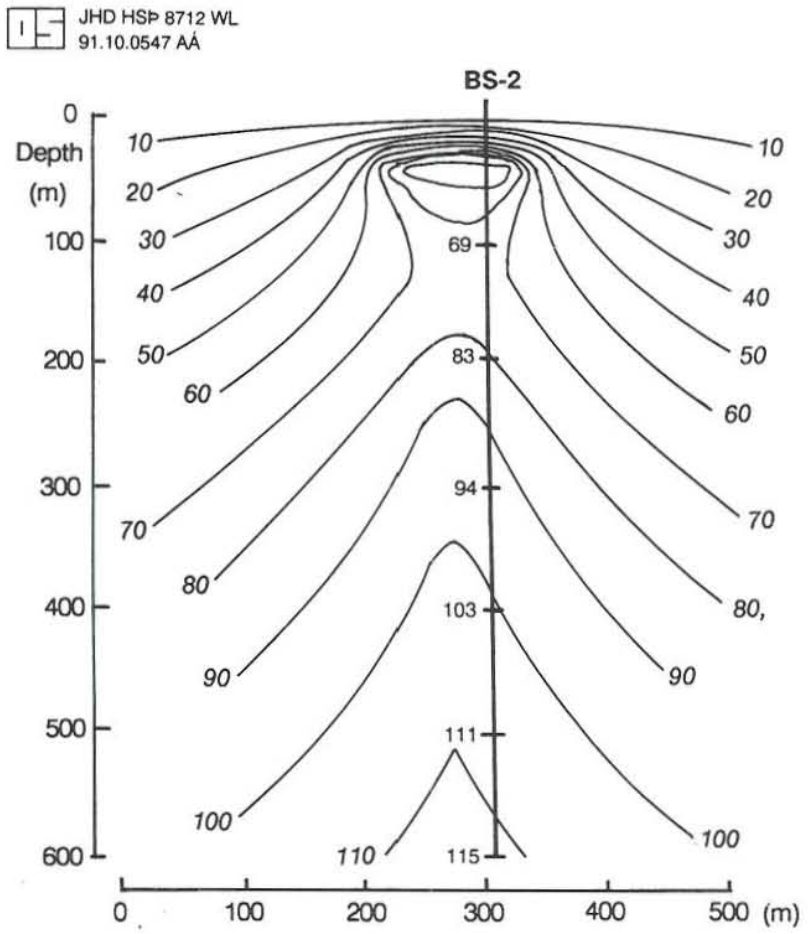

FIGURE 23: Temperature distribution resulting from Model 3

Figure 23 represents the temperature distribution resulting from Model 3 by VARMI. At well BS-2, calculated temperatures are satisfactorily consistent with the measured temperatures. So, we can say that although Model 3 is of less importance than Model 2, the simulated result of Model 3 also bears out that the conceptual model developed earlier is reasonable for describing the cause of the Bodmodsstadir geothermal field.

4.5 Results of the steady-state simulation

From the steady-state simulation by the VARMI program, we can make the following conclusions:

1. The conceptual model reasonably describes the natural state of the Bodmodsstadir geothermal field.

2. The supposed fracture seems to be dipping 8° towards well BS-10 and striking N40°E.

3. The bottom of well BS-10 is very close to the fracture.

4. Models 2 and 3 can be used to construct the initial model for the PT program.

5. NON-STEADY-STATE SIMULATION OF THE TEMPERATURE DISTRIBUTION

The steady-state simulation has shown that the conceptual model of the Bodmodsstadir geothermal system is acceptable. But it did not take time dependence into account and does not show the physical behaviour of the system in detail. In general, mass transport and convective and conductive heat transfer are important physical processes in geothermal systems. The Bodmodsstadir geothermal system consists of a hot water upflow through a nearly vertical fault, and the physical process is dominantly convective transport of mass and energy. A simple two dimensional distributed-parameter model was developed and is described in this chapter. It was calibrated by solving numerically both the mass and the energy transport equations with the program PT. By this, the physical processes and natural state of the Bodmodsstadir geothermal system are understood and we can get more useful information about the evaluation of the geothermal resources of this system and for planning its utilization.

5.1 Governing equations and solution method

5.1.1 Governing equations

In the last decade, rapid advances in the development of numerical simulators for modelling the behaviour of geothermal systems have been made (Bodvarsson et al., 1986). A numerical simulator, called PT, was completed by G.S. Bodvarsson (1982) at Lawrence Berkeley Laboratory. The PT simulator describes the physical processes by numerically solving both mass and energy transport equations for a liquid saturated medium. Using the Integrated Finite Difference Method (Edwards, 1972; Narasimhan and Witherspoon, 1976), the continuous equations governing the energy and mass transport in the saturated medium can be discreted in the forms of Equations 2 and 3:

Mass balance:

$$(V\phi\rho)_n \left[\beta_t \frac{\Delta P}{\Delta t} - \alpha_t \frac{\Delta T}{\Delta t}\right] = \sum_m \left(\frac{k\rho A}{\mu}\right)_{n,m}$$

$$\times \left[\frac{P_m - P_n}{D_{n,m} + D_{m,n}} - \eta_g \rho_g g\right] + (G_f V)_n \qquad (2)$$

Energy balance:

$$[(\rho c)_M V]_n \frac{\Delta T_n}{\Delta t} = \sum_m \left[\frac{(\lambda A)_{n,m}}{D_{n,m} + D_{m,n}} (T_m - T_n) + \right.$$

$$\left. \left(\frac{\rho_w c_w A k}{\mu}\right)_{n,m} (T_{m,n} - T_n) \left(\frac{P_m - P_n}{D_{n,m} + D_{m,n}} - \eta_g \rho_g g\right)\right] + (G_h V)_n \qquad (3)$$

where:

A - surface area (m^2)
c - heat capacity (J/kg°C)
$D_{m,n}$ - distance from nodal point of node m to the interface (m) of nodal point n

$D_{n,m}$ - distance from nodal point of node n to the interface (m) of nodal point m
g - acceleration due to gravity (m/s^2)
G_f - mass source/sink (kg/m^3s)
G_h - heat source/sink (J/m^3s)
P - pressure (p_a)
T - temperature (°C)
V - volume (m^3)
ϕ - porosity
ρ - density (kg/m^3)
β_t - total compressibility (p_a^{-1})
α_t - total expansivity ($°C^{-1}$)
λ - thermal conductivity (W/m°C)
η_g - directional cosine for the gravity term
ρ_g - fluid density in the interface

$$\rho_g = \frac{1}{2}(\rho_m + \rho_n)$$

μ - dynamic viscosity (kg/ms)
k - absolute permeability (m^2)
$(\rho c)_M$ - integrated heat capacity for node m ($J/m^{3o}C$)

$$(\rho c)_M = \phi \rho_w c_w + (1-\phi)\rho_r c_r$$

w - fluid
t - time
m - node m
n - node n

These equations are valid for an arbitrary node n connected to an arbitrary number of nodes m. They can be combined for simultaneous solution into a single matrix equation.

$$[A]\{X\} = \{b\}$$

The coefficients in the matrix [A] are in general a function of the temperature and pressure and, therefore, the equations are nonlinear. The vector $\{X\}$ contains the unknowns [ΔP and ΔT] and vector $\{b\}$ represents the known explicit quantities. The sets of nonlinear equations are solved using an efficient direct solver (Duff, 1977) and an iterative scheme for the nonlinear coefficients (Bodvarsson, 1982). Basically, the solver uses LU decomposition and a Gaussian elimination procedure to solve a set of linear equations.

5.1.2 The distributed-parameter model

The conceptual model (shown in Figure 18) obtained from the geological structure, interpretation of temperature logs and the steady-state simulation, is divided into blocks to construct the distributed-parameters model. The grid, shown in Figure 24, is 1100 m long and 1000 m deep representing the central part of the grid used in VARMI. The grid consists of 11 layers and 11 columns, a total of 123 grid blocks which are smaller near the fault but become bigger away from the fault which, including the horizontal aquifers, is 20 m thick. As shown in Figure 24, the B columns and the C layer are the boundary blocks and are assigned big volumes. The shady area on Figure 24 represents the aquifers.

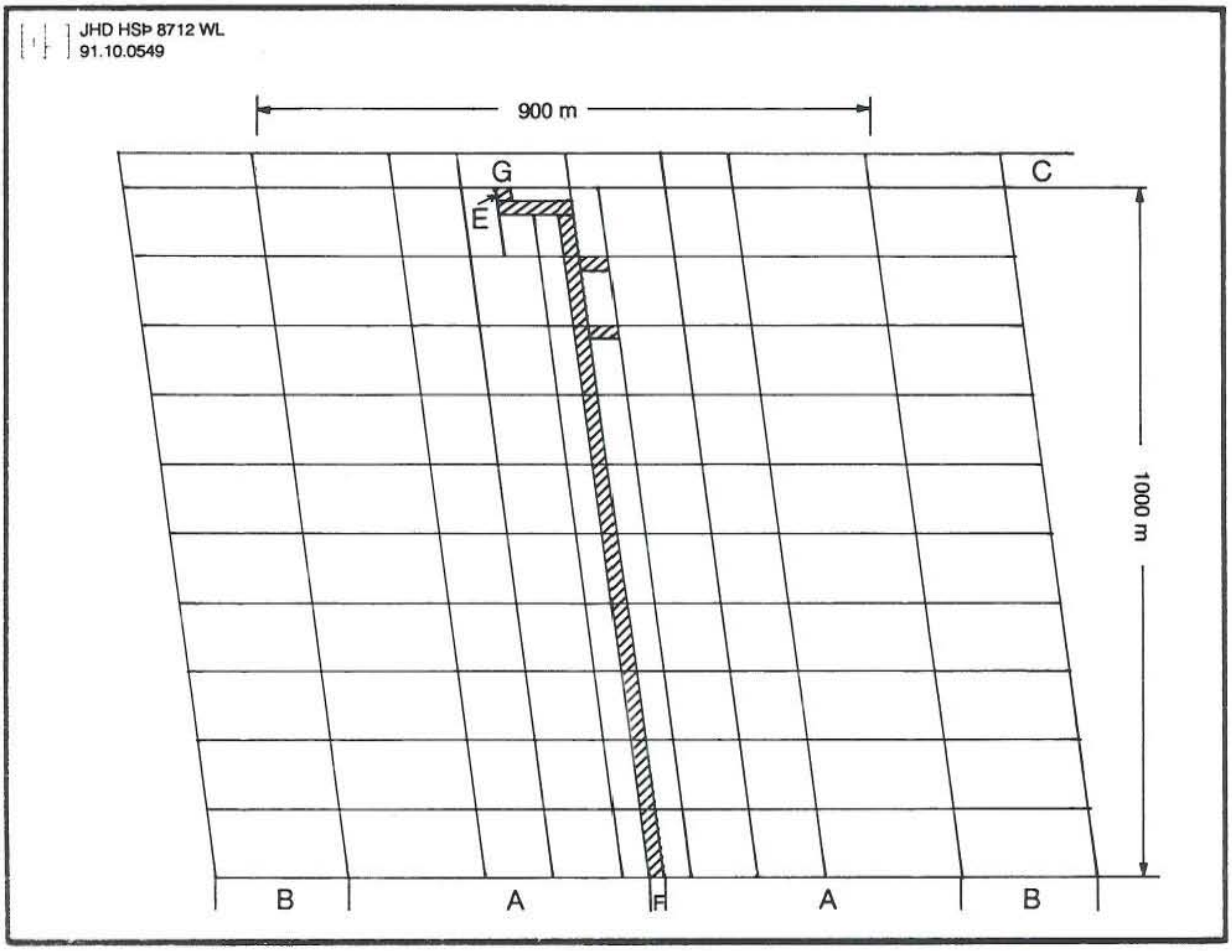

FIGURE 24: The grid for the PT simulator

In the model, each block is homogeneous and is distinguished by different physical parameters of the solid medium such as permeability, conductivity, porosity, density and specific heat capacity. The fluid compressibility is 5.0×10^{-10} P_a^{-1} in all the blocks, the heat capacity is 4200 J/kg°C and the density is temperature dependent.

The simulation was performed in two steps. First, only the energy equation was solved. In this part, the specific heat capacity was very high and the temperature of the blocks representing the fault and the aquifers was fixed to see how long time it took for the temperature to reach the quasi-steady-state (so-called natural state). In the second step the simulation was performed by solving both the mass and the energy transport equations. In this part, the permeability and conductivity of the aquifers and the rock matrix were gradually changed to match the temperature and pressure distributions in the reservoir, and to get an estimation of discharge and recharge before production. Table 4 lists the main parameters used in the simulations.

5.2 Simulation by solving only the energy transport equation

In the simulation where only the energy transport equation was solved, the aquifer blocks were assigned a very high specific heat capacity (1×10^6 J/kg°C) and all the blocks were given low

porosity and permeability values (Table 4). The conductivity of the basaltic rocks is given at 1.9 W/m°C according to Oxburgh and Agrell (1982). The conductivity of the fault is estimated to be 4.0 W/m°C. The volume of the boundary blocks are of the order of 10^8 m^3. The initial temperature was assumed to be 4°C at the surface (mean annual temperature) and the temperature gradient was set at 126°C/km, same as in the steady-state simulation. The initial pressure at each block was equal to the sum of the atmospheric pressure and the weight of the water column from the surface to the geometrical centre of each block. The temperature and pressure in the top layer (C) were assumed to be 4°C and 1 bar, respectively.

TABLE 4: Main parameters used in the non-steady-state simulations

	Only energy equation	Energy and mass equations
fluid	$\beta = 5\times10^{-10}$ P_a^{-1} c = 4200 J/kg°C	same same
rock	λ_f = 4.0 W/m°C λ_m = 1.9 W/m°C ϕ = 0.05 c = 10^6 J/kg°C k = 10^{-18} m^2	same same ϕ_f = 0.2, ϕ_m = 0.05 c = 900 J/kg°C $k_f = 10^{-13}$ m^2, $k_m = 10^{-18}$ m^2
initial conditions	4°C surface temperature 126°C temperature gradient 1 bar surface pressure hydrostatic pressure	same same same same
block F	no	T_o = 130°C P_o = 106 bar

* subscripts "f" and "m" mean "fault" and "matrix", respectively.

Temperature distributions using different simulation times are presented in Figures 25 - 28.

Temperature distributions after 500 years and 1000 years simulation time are plotted in Figure 25. Significant differences can be seen between the distributions, especially in the vicinity of the fault. The temperature distributions after 1000 years and 2500 years (Figure 26) have the same features as the one in Figure 25. This shows that the temperature needed at least 2500 years after the fault was created to reach quasi-steady state.

Figure 27 shows the temperature distribution after 2500 years and 5000 years. The differences between the two distributions is smaller than in the previous figures and in Figure 28 there is almost no difference between the temperature distribution after 5000 years and 10,000 years.

It can be concluded from these calculations that the temperature in a simple geothermal system, such as the Bodmodsstadir geothermal system governed by hot fluid upflow, reaches quasi-steady state in 5000 years.

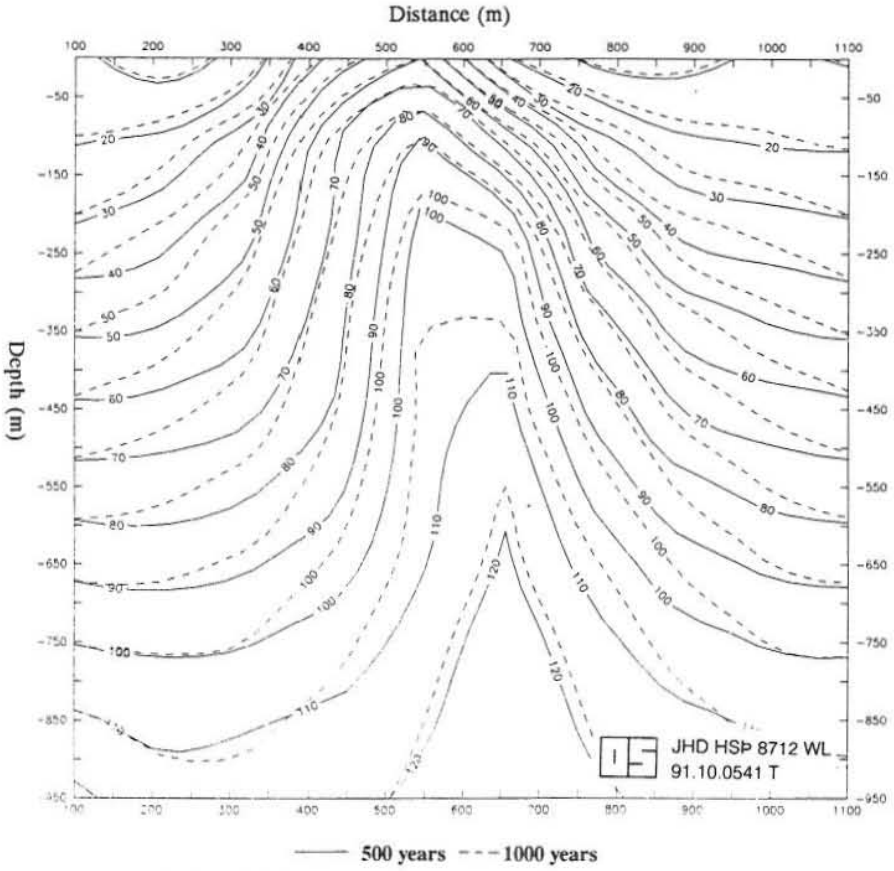

FIGURE 25: Temperature distributions calculated after 500 and 1000 years simulation time

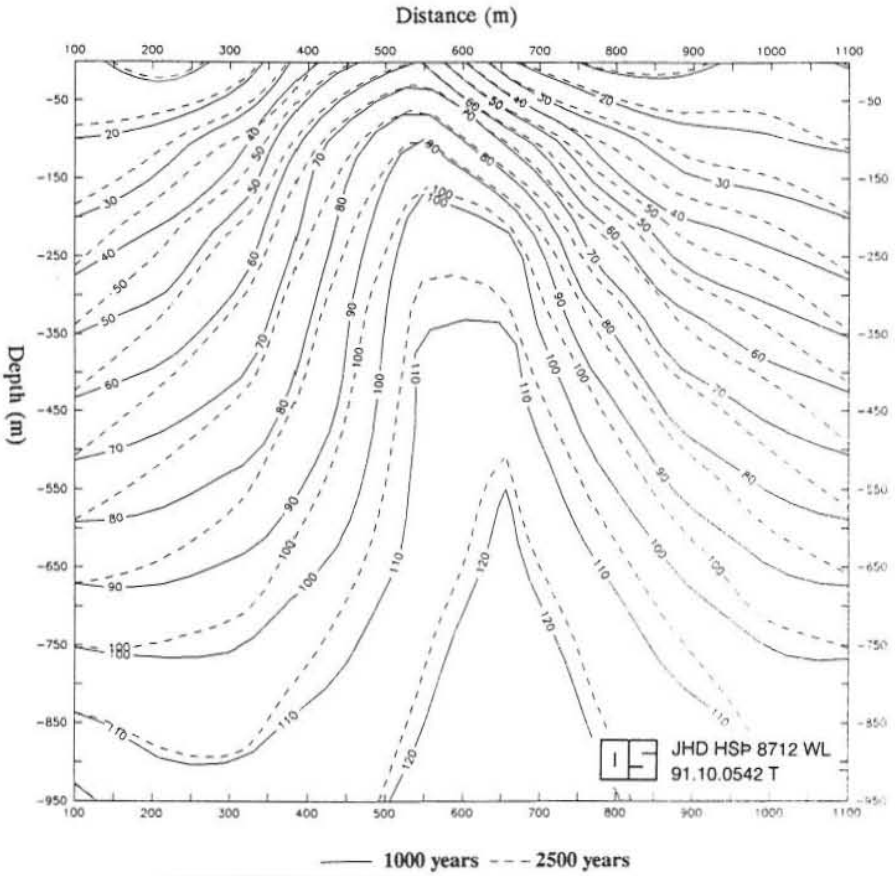

FIGURE 26: Temperature distributions calculated after 1000 and 2500 years simulation time

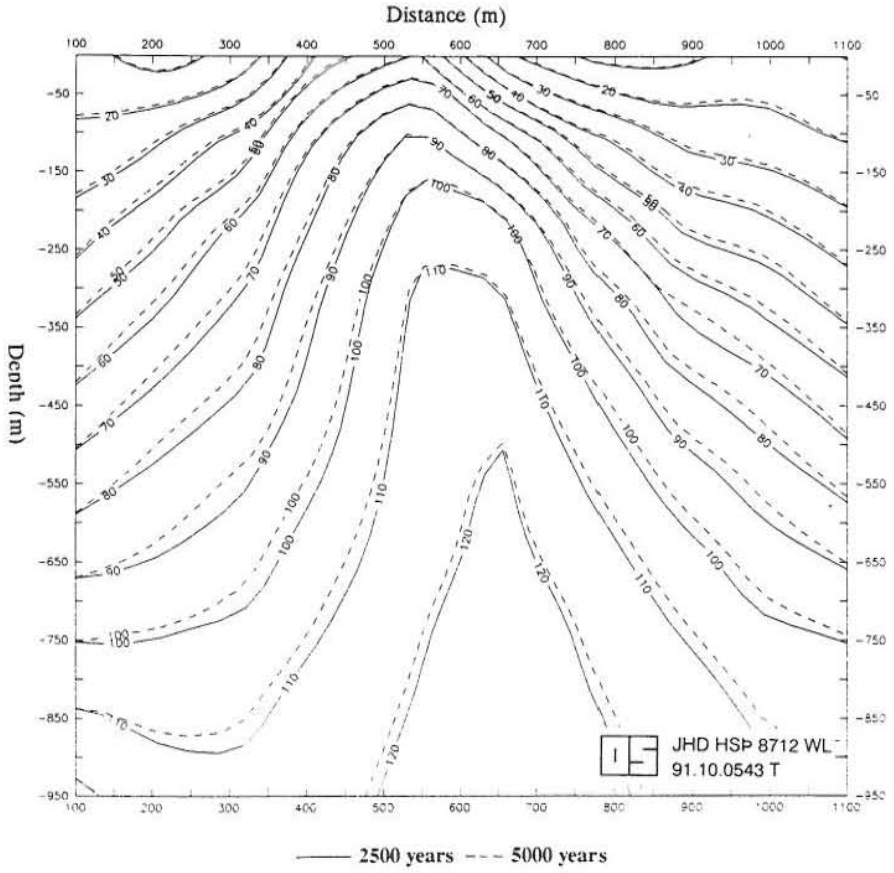

FIGURE 27: Temperature distributions calculated after 2500 and 5000 years simulation time

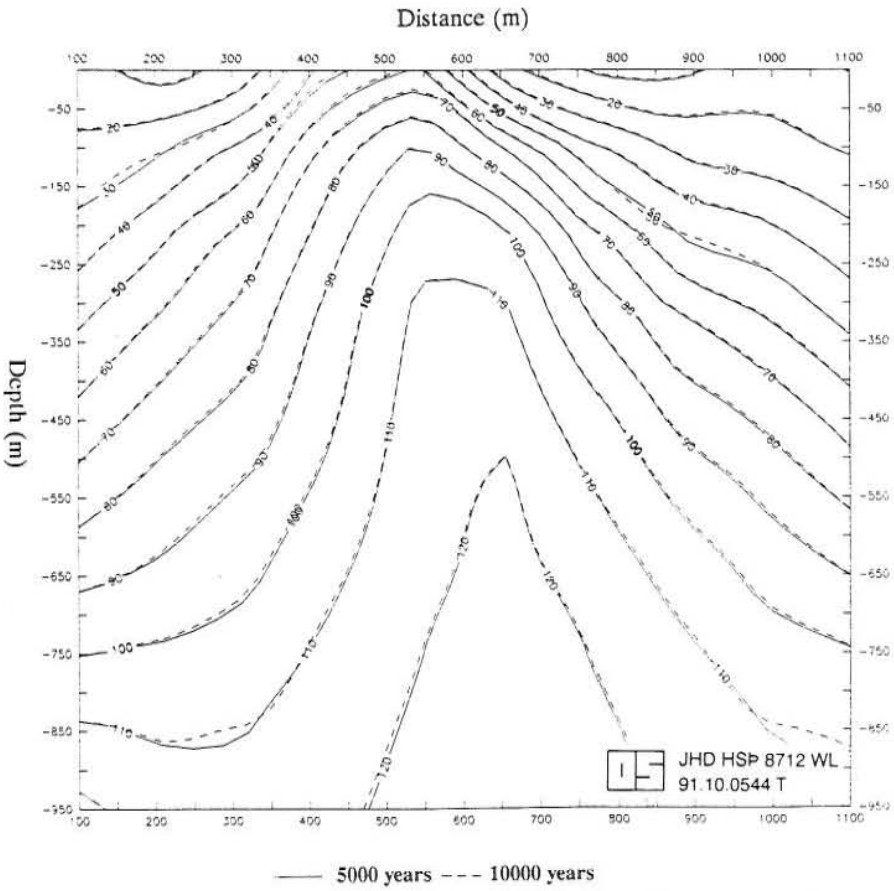

FIGURE 28: Temperature distributions calculated after 5000 and 10,000 years simulation time

5.3 Simulation by solving both the energy and the mass transport equations

In the simulation where both the mass and the energy transport equations were solved, the initial temperature and pressure, properties of the fluid and thermal conductivity are the same as in Section 5.2 (Table 4). An additional big boundary block F (Figure 24) controlling the recharge of hot fluid from depth into the fracture (aquifer) is put at the bottom of the fault. This block has the same permeability and porosity as the fault, but higher pressure and temperature which were adjusted in the simulation. Block E (Figure 24) has the same properties as the fault so that discharge can pass through it to the surface, and block G is assigned large volume and can store the natural discharge.

The permeability and porosity of the aquifers and the temperature and pressure of block F are adjusted by running the PT simulator. In general, the permeability of the aquifers greatly affects the temperature distribution and the flowrates of the recharge and the discharge, but the conductivity and porosities have no obvious influence on the simulated results.

Figure 29 represents the temperature distribution after 5000 years. The essential character of the distribution is very similar to the results from the steady-state simulation (Figure 21) and to the simulation calculated using only the energy equation. Figure 30 shows the comparison between the calculated and observed temperature at wells BS-2 and BS-10. The difference between the calculated temperature and the observed temperature is very small at well BS-10, but there is a significant difference in the upper part of well BS-2. It is difficult to fit the temperature reversal into a two-dimensional simulation by PT, partly because the blocks are too large. From Figure 29 and 29, we can say that the calculated temperature roughly fits the observed ones.

Figure 31 shows the temperature and pressure in the block representing the horizontal aquifer at 30 m depth. At that depth, the calculated temperature is 96°C and the pressure is 4.1 bar. Wells BS-1 and BS-2 were drilled through this aquifer. Both wells are self-flowing and producing from this aquifer. The measured temperature of this aquifer is about 95°C. So, there is no difference between observed and calculated pressure and temperature in this block.

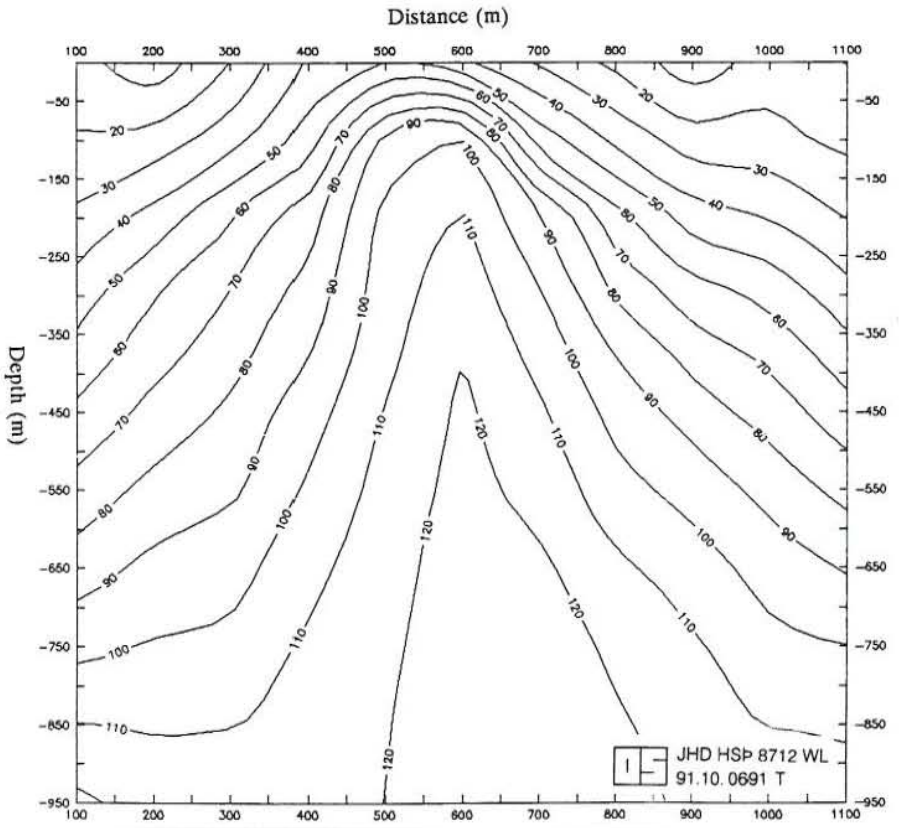

FIGURE 29: Temperature distribution calculated from solving both the mass and the energy transport equations

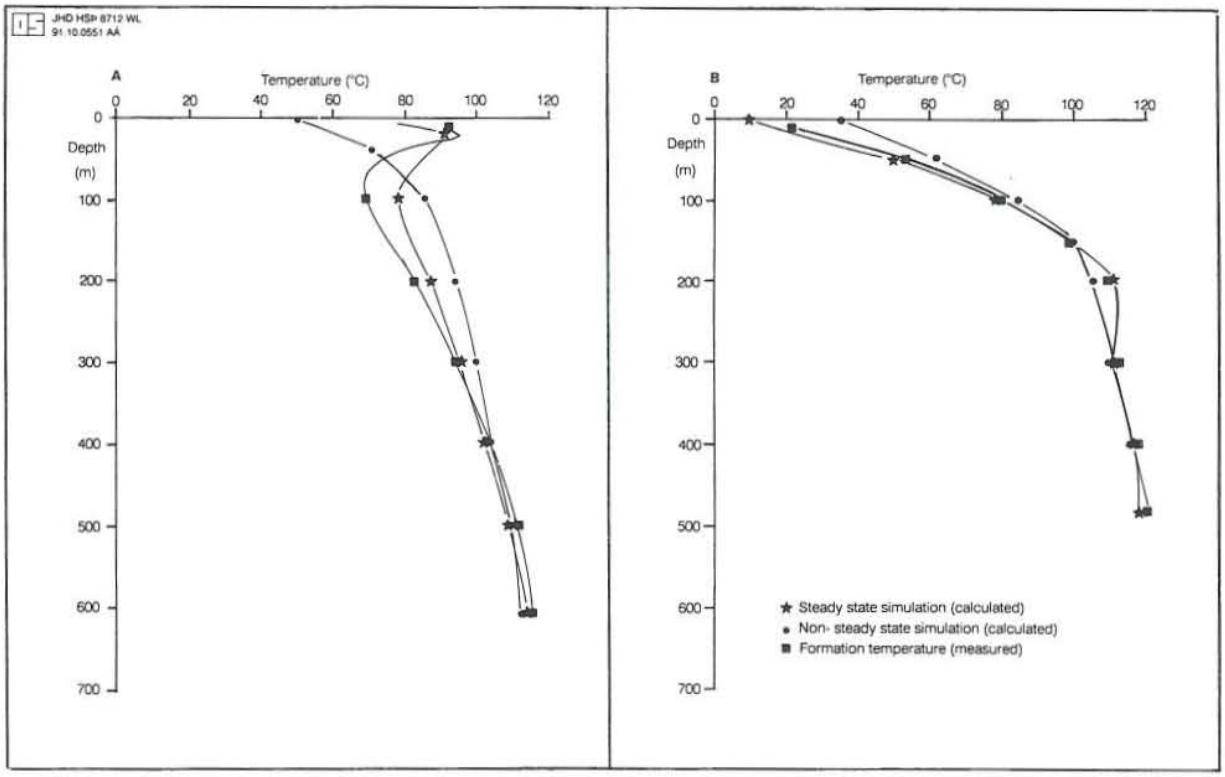

FIGURE 30: Comparison between observed and calculated temperature in BS-2 (A) and BS-10 (B)

Figures 29-31 present the best results from the simulation. In this case, the permeability of the aquifer and the rock matrix is 1.0×10^{-13} m^2 and 1.0×10^{-18} m^2, respectively, and the porosity of the fault is 0.2. The temperature and pressure in block F are 130°C and 106 bar, respectively, and both the recharge from block F and the discharge from block E are more than 1.0 kg/s. In the simulation, the rate of the discharge is lower than the natural discharge, which is about 2.0 l/s from the hot springs (Olafsson, 1967) plus the flow into the river. The discharge rate of 10 kg/s can be obtained when the permeability of the fault is given as 8.0×10^{-13} m^2 in the simulation, but then the calculated temperature above 100 m depth is higher than the observed temperature.

5.4 Results of the non-steady-state simulation

In summary, two conclusions may be drawn from the non-steady-state simulation.

1. A simple geothermal system like Bodmodsstadir, created by hot fluid upflow through a fault, reaches quasi-steady-state (natural state) in about 5000 years.

2. The temperature distribution in the Bodmodsstadir geothermal system depends strongly on the rate of the hot upflow and the permeability of the fracture striking NE and dipping 8° (if 1.0 kg/s of 130°C hot water flows up through the fault with 1.0×10^{-13} m^2 permeability, the temperature distribution after 5000 years simulation times is close to the observed formation temperature distribution).

The natural state model of the Bodmodsstadir geothermal system, developed here, may be used further to evaluate the geothermal resources of this system and for planning its development.

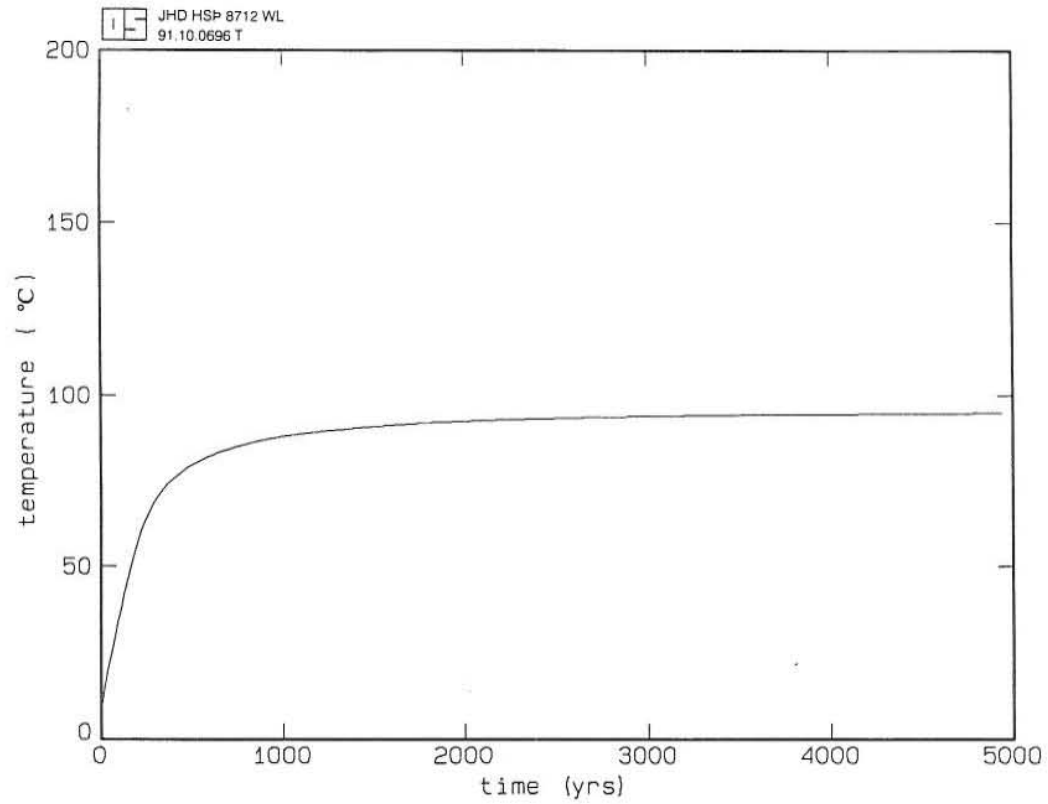

A

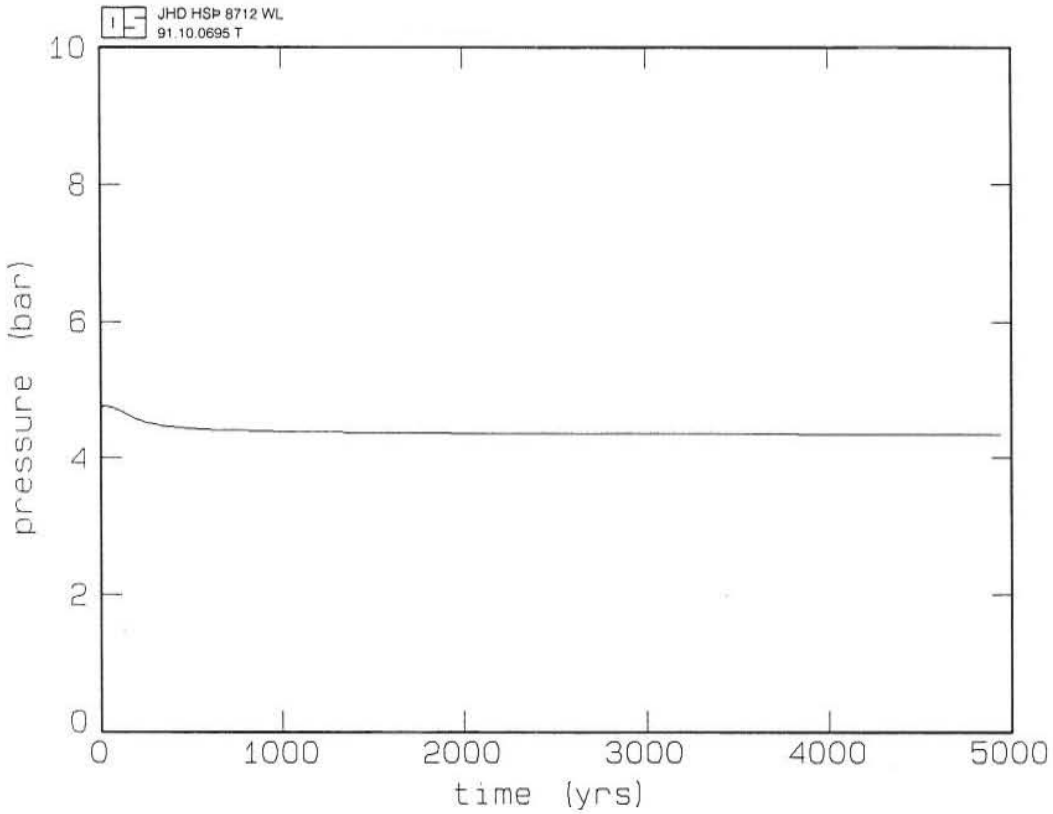

B

FIGURE 31: Calc. temperature (A) and pressure (B) in the horizontal aquifer at 30 m depth

6. CONCLUSIONS AND RECOMMENDATIONS

The main conclusions of this study may be summarized as follows:

1. The Bodmodsstadir geothermal field is a simple geothermal system consisting mainly of a fracture from which hot water flows to the surface. Based on the integrated interpretation of temperature logs, surface temperature measurements, water level and pressure data from this area, the fracture is striking NE and dipping to the NW.

2. The best model in the steady-state simulation gives about 8° dip angle for the fault.

3. The non-steady-state simulation shows that it takes about 5000 years for the Bodmodsstadir geothermal system to reach quasi-steady-state conditions.

4. The permeability of this fault is 0.1 - 0.8 Darcy and the recharge from depth is 1.0 - 10.0 kg/s.

5. The natural state model developed in this study could be used to evaluate the geothermal system and for planning its utilization.

The following suggestions are made:

1. To drill one or two shallow boreholes (about 80 m deep) between wells BS-10 and BS-8 to determine the extent of shallow horizontal flow of hot water and thereby better locate the upflow zone.

2. If the data from the suggested shallow boreholes support the present model, it is recommended to deepen well BS-10 to 600 - 800 m depth. An alternative new 300 - 500 m deep borehole could be drilled between wells BS-2 and BS-10, approximately 40 m south of well BS-10.

3. If the suggested shallow borehole(s) indicate lateral flow from NNE, the next deep borehole should be drilled NNE of well BS-10.

ACKNOWLEDGEMENTS

It gives me a great pleasure to express my gratitude to Dr. Ingvar B. Fridleifsson, the director of the UNU Geothermal Training Programme, for providing excellent work conditions during my studies.

I wish to thank Helga Tulinius and Olafur G. Flovenz first, my advisors, for their great help and critical advice during all stages of the data analysis and preparation of this report.

My thanks go to Valgardur Stefansson, Benedikt Steingrimsson, Omar Sigurdsson, Ludvik S. Georgsson, Grimur Bjornsson, Gudni Axelsson, Marcia Kjartansson and all the staff at Orkustofnun for their help.

I will always be indebted for what they have done, and I intend to do much more in geothermal research of China upon my return.

REFERENCES

Bodvarsson, G.S., 1982: Mathematical modelling of the behaviour of geothermal systems under exploitation. Ph.D. thesis, Lawrence Berkeley Laboratory, University of California, Earth Sciences Division, 353 pp.

Bodvarsson, G.S., Pruess, K., Stefansson, V., and Eliasson, E.T., 1984: The Krafla geothermal field, Iceland. Part 2: The natural state of the system. Water Resour. Res., 20, 1531-1544.

Bodvarsson, G.S., Pruess, K., and Lippmann, M.J., 1986: Modelling of geothermal systems. Jour. of Petrol. Techn., 38, no. 10, 1007-1021.

Bodvarsson, G.S., Bjornsson, S., Gunnarsson, A., Gunnlaugsson, E., Sigurdsson, O., Stefansson, V., and Steingrimsson, B., 1990: The Nesjavellir geothermal field, Iceland. Part 1: Field characteristics and development of a three-dimensional numerical model. Geotherm. Sci. & Tech., 2 (3), 189-228.

Duff, I.S., 1977: MA28 - a set of FORTRAN subroutines for sparse asymmetric linear equations. AERE, report R8730, Harwell, Great Britain.

Edwards, A. L.,1972: TRUMP: A computer program for transient and steady state temperature distribution in multidimensional systems. Lawrence Livermore Laboratory, Livermore, California.

Flóvenz, O.G., 1985: Application of subsurface temperature measurements in geothermal prospecting in Iceland. Jour. of Geodynamics, 4, 331-340.

Flovenz, O.G., Georgsson, L.S., and Arnason, K., 1985: Resistivity structure of the upper crust in Iceland. Jour. of Geophy. Res., 90, B12, 10136-10150.

Icelandic Drilling Company, 1991: Drilling reports (in Icelandic).

Narasimhan, T.N., and Witherspoon, P.A., 1976: An integrated finite difference method for analyzing fluid flow in porous media. Water Resources Research, 12, 1, 57-64.

Olafsson, Th., 1967: Discharge measurements in Arnessysla and Rangarvallasysla in June and July, 1967. Orkustofnun, report (in Icelandic), Reykjavik, 28 pp.

Oxburgh, E.R. and Agrell, 1982: Thermal conductivity and temperature structure of the Reydarfjordur borehole, Jour. of Geophy. Res., 87, B8, 6423-6428.

Palmason, G., 1973: Kinematics and heat flow in a volcanic rift zone, with application to Iceland, Geophys. J. R. Astr. Soc., 33, 451-481.

State Drilling Contractors, 1974: Drilling reports (in Icelandic).

Thorbergsson, G., 1991: Boreholes at Bodmodsstadir. Orkustofnun, report GTh-91/02, (in Icelandic).